CHARACTERIZATION, QUANTIFICATION, AND RECOVERY OF RARE EARTH ELEMENTS(REES) IN SOUTH AFRICAN COAL FLY ASH SAMPLES

By

TSHILIDZI MICHAEL RAMPFUMEDZI

1101203

A Master's dissertation submitted to the University of the Witwatersrand in fulfillment with the requirements of the degree of Master of Science.

SUPERVISOR: PROF. LUKE CHIMUKA

CO-SUPERVOSOR: DR JAMES TSHILONGO

March 2024

DECLARATION

Upon submitting this dissertation, I declare that I worked independently, with the assistance of my supervisor, Prof. Luke Chimuka, and Dr James Tshilongo as my co-supervisors. The citations have been included, and the knowledge obtained from existing literature has been fully recognized within the text. This research is being submitted as part of the requirements for a master's degree in chemistry at the University of the Witwatersrand. It has not been previously submitted for any other academic qualification or examination.

_____

(Signature of candidate)

05 day of March 2024 at Randburg

ABSTRACT

Rare earth elements (REEs) are naturally distributed throughout the Earth's crust, typically in low concentrations. They are not typically found in isolation but are rather present in various minerals, often in amounts too minute for cost-effective extraction. Fly ash is among the sources that are deemed economically viable for extracting REEs.

The objective of this study was to create environmentally sustainable approaches for measuring and reclaiming rare earth elements (REEs) in coal fly ash (CAF) samples. The study involved analyzing fly ash samples collected from various coal power stations using a range of standard and advanced techniques, including X-ray fluorescence (XRF), X-ray diffraction (XRD), scanning electron microscopy (SEM), and inductively coupled plasma mass spectrometry (ICP-MS) and inductively coupled plasma optical emission spectrometry (ICP-OES).

The XRF only shows the presence of REEs from all three fly ash samples with a range of 40 to 100 ppm and mineral oxide ranging from 0.1 to 50 %. The XRD results show that fly ash sample is a siliceous-rich sample with abundant minerals such as quartz (SiO_2), magnetite (Fe_3O_4), and mullite ($Al_{4.52}Si_{1.48}O_{9.74}$). The SEM analysis of the sample confirmed the presence of rare earth minerals, including monazite which is a light atomic mass (LREE), xenotime, a heavy atomic mass (HREE), and perrierite-bearing minerals.

The results obtained from the instrumental analysis show that the ICP-MS instrument is the more effective analytical technique for REE analysis in this context as compared to ICP-OES. Using certified reference materials, the results obtained by two acids digestion technique, acids digestion and sodium peroxide fusion in, CGL 111, CGL 124, and AMISO276, were

compared to validate whether the methods are reliable. The acid digestion approach demonstrated greater effectiveness in comparison to the sodium peroxide fusion method.

The recovery percentage (%) from ICP–MS showed an excellent percentage yield (80 – 120%) compared to the ICP–OES instrument (50 – 120%). The ICP–MS data indicate that all fly ash samples have a high concentration of LREEs and a lower concentration of HREEs. Excellent recovery was obtained by ICP–MS in a developed microwave acid digestion method. The concentration of REEs obtained from ICP - MS and OES in fly ash samples ranged from 50 ppm to 200 ppm for light rare earth elements and 0.5 ppm to 20 ppm for heavy rare earth elements. The total REE (TREE) concentrations in all fly ash samples range from 400 ppm to 600 ppm.

Keywords: REEs, fly ash, multi-acid digestion, fusion

ACKNOWLEDGEMENTS

First, I would like to express my gratitude to the Almighty God, who gave me strength and showed His grace to sustain me through out this study.

I would like to extend my profound thanks and heartfelt gratitude to my supervisor, Professor Luke Chimuka, and my co-supervisor, Dr. James Tshilongo, for their unwavering support, patience, guidance, and inspiration during this research. Your wisdom and encouragement have enriched my academic journey and played a pivotal role in shaping me into a better individual in both life and academia. My appreciation knows no bounds.

I would also like to extend my gratitude to my fellow analytical chemistry division (ACD) postgraduate team and researcher for their support and guidance. I would also like to extend my gratitude to ACD management and team for their support throughout the studies and Mintek for the financial support they put through the study.

Lastly, I would like to give thanks to my family and friends who have supported me in pursuing my studies and their words of encouragement.

Contents
Pages

List of Tables

List of Figures

ABBREVIATIONS

$(NH_4)_2SO_4$	: Ammonium sulphate
$Al_2\ O_3$	: Aluminium Oxide
CaO	: Calcium oxide
$CaSO_3$	: Calcium sulphite
CCPs	: Combustion by-products
CFA	: Coal fly ash
CRMs	: Certified Reference Materials
D_2EHPA	: Bis (2-ethylhexyl) phosphoric
DOE	: Department of Energy
Eu	: Europium
$Fe_2\ O_3$	: Iron Oxide
Hf	: Hydrofluoric acid
HREE	: Heavy rare earth elements
ICP-MS	: Inductively coupled plasma - mass spectrometry
ICP-OES	: Inductively coupled plasma - optical emission spectrometry
INAA	: Instrumental neutron activation analysis
LED	: Light-emitting diode
LREE	: Light rare earth elements
MW-AAE	: Microwave-assisted acid extraction
Na_2CO_3	: Sodium carbonate

Na_2O_2 : Sodium Peroxide

NaOH : Sodium hydroxide

NET : National Energy Technology Laboratory

Ppb : Parts per billion

Ppm : Parts per million

R&D : Research and development

REEs : Rare earth elements

REY : Rare earth elements

SARM : South African Reference Material

Sc : Scandium

SEM : Scanning electron microscope

SEP : Sequential extraction procedures

SiO_2 : Silicon dioxide.

Sm : Samarium

TGA : Thermogravimetric analysis

WDXRF : Wavelength dispersive X-ray fluorescence spectrometry

EDXRF : Energy dispersive X-ray fluorescence

XRD : X-ray diffraction

XRF : X-ray fluorescence

PV : Photovoltaics

MW : Megawatt

CHAPTER 1: INTRODUCTION

The dissertation entitled "**Characterization, quantification, and recovery of Rare Earth Elements (REE) in South African Coal Fly Ash Samples"** is divided into six chapters.

This first chapter examines explicitly the background of the study, together with the study's objectives, problem statement, motivation, hypothesis, and research questions.

1.1. Background

Rare earth elements (REEs) are elements that exist in the Earth's crust and are found in low concentrations. These elements are mostly separated into different minerals in which they exist; in most cases, their concentration is too small for economical extraction. REEs are the 15 lanthanide series elements (elements 57-71) as well as scandium (21) and yttrium(39). REEs are used in different industrial processes; these elements are considered important elements in terms of the production of green technology and electronics appliances, and they are also in the medical and defense industries (Scott et al. 2015). They have been recognized as being important in research and development (R&D) for several scientific and commercial applications. Coal and coal byproducts such as ash and other waste materials have been found to contain REEs in varying amounts and concentrations.

The demand pick for REEs in the current market is higher than the supply pick, which is growing steadily as well. As the world is shifting towards carbon footprint-free, the production of green clean energy and technology is expected to guide the demand for REEs (MINERAL 2010). REE consumption is anticipated to be guided by demand for green technology, such as wind turbines and other technology production that uses permanent magnet products. Since REEs are isolated according to their characteristics, their supply and demand chains vary, and the levels at which they are found differ according to their mining sites. The South African economy holds a bright, promising future regarding REE production. This is because the South African economy depends much on the coal mining industry to generate energy (January 2017).

Rare earth elements can be grouped into different groups due to their abundance and chemical properties. Elements with lower atomic mass numbers (57 – 62) from samarium to lanthanum are grouped as light rare earth elements (LREEs), while elements with atomic numbers (63 – 71)

from europium to lutetium are referred to as heavy rare earth elements (HREEs).

However, elements such as yttrium, which fall between LREEs and HREEs, are called (mid-REEs); nonetheless, due to their chemical similarity, which is almost the same as that of HREEs, they are grouped with HREEs. HREEs exist in small quantities in nature with approximately 130,000 tonnes, making them extremely difficult to determine and requiring multiple intensive processing steps for purification (Mehmood 2018). Consequently, this makes them more expensive from the value of chain perspective.

Residual fly ash is saturated with organic materials from the flue gases of furnaces at pulverized coal power plants. Burning coal in any pulverized coal boiler produces minerals that are retained from coal, and those minerals are converted into chemical species that are chemically reactive or could be chemically activated. At varying concentrations, REEs can be found in coal byproducts, including ash, coal-related sludge, and mine drainage. There is a possibility that some coal ash contains a higher percentage of heavy (generally more valuable) REEs compared to natural ores (Peterson et al. 2017).

Coal fly ash is regarded as a significant potential source of REEs because it is retained during coal combustion for energy generation, and large quantities of coal fly ash are stored for future use worldwide. Fly ash is categorized based on its properties and weight composition, falling into two main classes: cementitious and pozzolanic. Cementitious fly ash is designated Class C and consists of a minimum of 50% by weight of SiO_2 + Al_2O_3 + Fe_2O_3. In contrast, pozzolanic fly ash, known as Class F, contains more than 70% by weight of SiO_2 + Al_2O_3 + Fe_2O_3 in its composition (Landman 2003).

Determination of REEs is extremely challenging either by extraction methods or by instrumental techniques because REEs have low concentrations that are mixed with other minerals due to their chemical

similarity. Recent studies in fly ash have concentrated on determining trace element concentrations and leaching effects by inductively coupling plasm-optical emission spectroscopy (ICP–OES), gas chromatography-mass spectrometry (MS), and X-ray fluorescence (XRF) to mass spectrometry using laser ionization (Zhang, Yang, and Honaker 2018).

1.2. Problem Statement

South Africa is one of the countries that has a large amount of coal, hosting almost 6% of the world's coal. Approximately 95% of electricity in South Africa is generated by coal, making the demand for coal supply high, as it is the mainstream of the economy and the country. Globally, the demand for coal continues to increase for the generation of energy and electricity from coal combustion. The retained coal fly and bottom ash from coal combustion must be managed well in terms of handling and storage because they can have several effects, such as environmental impacts on soil, air, and water, and they can also be hazardous to living organisms (Wagner and Matiane 2018a). Numerous sample analyses show that the REE content is comparable to some conventional ores.

Therefore, there is a need to implement new strategies and methods for utilizing coal fly ash (CFA) and consequent reduction. The fly ash generated is used for making cement in the construction industry; however, much more fly ash is produced than is needed. On average, 25% of the fly ash generated is utilized worldwide; therefore, there is a need to find alternative applications for extra-wrapped fly ash. Almost 50 million tons of ash are produced annually in South Africa, but only 10% is utilized (Al 2018; Franus et al. 2015)

1.3. Motivation for research

The exploration of fly ash as a viable source of rare earth elements (REEs) is a relatively recent area of research that has garnered significant global attention and investment. Among their uses, REEs are notably incorporated

into many new technologies for energy, such as fuel cells, green energy devices, solar panels, and wind motors (Wdowin 2015). It will be valuable for the industry to recover REEs from coal fly ash, which is generated at coal-fired power plants and left unused by the plants. As a result, a significant amount of value will be added to the industry by recovering REEs from coal fly ash.

While fly ash is a potentially new source of rare earth elements, in most conventional mines, only a few of these minerals can be extracted. Consequently, fly ash generated by coal plants worldwide is increasing, and recycling and utilizing these materials has become increasingly essential. Therefore, the research community and industry are exploring methods to extract REEs from coal-derived fly ash economically. Additionally, limited literature on REEs in South African coal and related products appears.

1.4. Aim and Objectives

1.4.1. Aim

This research aimed to quantitatively determine and recover REEs present in coal fly ash using various analytical techniques.

1.4.2. Objectives

Specific objectives were to:

- Develop a microwave-based sample preparation method prior to the quantitative determination of total REEs in CFA samples using inductively coupled plasma techniques (ICP–OES/ICP–MS). This objective was covered by the following activities
    - Optimization of samples, microwave temperatures, digestion times, and reagent concentrations was carried out using multivariate mathematical tools.

- Certified reference materials were used to investigate the analytical merits of the method (detection limits, accuracy, linearity, precision, and accuracy).
- Optimal parameters were applied to real CFA samples to obtain the best results.

- Investigate the Recovery of REEs in CFA samples using leaching and precipitation reagents. This objective was covered by the following activities;
  - Exploration of various parameters (mass, type of leaching solvent and volume, precipitation reagent type and volume, extraction time, etc.) was used to determine which factors affect the extraction and precipitation efficiency of the REEs.
  - Validation of the recovery methods using certified reference materials.
  - Application of the optimum parameters in CFA samples.

1.5. Research Hypothesis and Questions

1.5.1. Hypothesis

- The recovery of REEs in coal fly ash samples by the microwave-assisted base sample preparation method is rapid and its yields ~100% recoveries.

1.5.2. Questions

- What minerals are present in the South African coal ash samples that may contain REEs?

- Which sample preparation method recovers the highest level of REEs, multi-acid digestion or sodium peroxide fusion?
- Which technique will recover the concentration of REEs with high accuracy and precision between ICP–MS and ICP–OES?

1.6. Outline of dissertation

Chapter One: Introduction

This chapter provides a brief background of the study. It also gives a quick overview of the problem statement, motivation for the study, aims, and objectives with research questions.

Chapter Two: Literature review

This chapter reviews how fly ash occurs and is produced and the importance of fly ash and REEs. It also provides an overview of literature reviews for techniques and other studies.

Chapter Three: Methodology

This chapter provides comprehensive details regarding the materials and methods employed to accomplish the specified objectives of the study.

Chapter Four: Results and Discussion

This chapter briefly discusses and presents results obtained through XRF, XRD, SEM, ICP–MS, and ICP–OES techniques from all preparation methods.

Chapter Five: Conclusion and Recommendation

This chapter covers an overview and findings of the study and gives a conclusion and recommendation based on the results.

CHAPTER 2: LITERATURE REVIEW

This chapter provides an overview of coal ash, the processes involved in forming coal, its production methods, economic significance, and various applications. Additionally, it gives an overview of the coalfields in South Africa. The chapter also discusses the analytical techniques used in this study to measure minerals and REEs in coal combustion products, including XRF, XRD, SEM, ICP–OES, and ICP–MS.

2.1. Introduction of coal ash

Coal ash is the residue that is produced during coal combustion; these include solid residues or materials produced by coal combustion, such as fly ash, bottom ash, and boiler slag, which are classified as coal ash. Frandsen (1997) stated that during the thermal conversion of coal, there are ash-forming species that are likely to form ash, which can produce ash that appears as fly ash, bottom ash, or deposits as a result of the thermal conversion of coal. (1997) Typically, inorganic constituents (noncombustible) are incorporated into coal or are introduced with coal during the combustion process (e.g., dirt, clay). Ash is made up of these constituents. Coal is typically characterized by inorganic constituents and oxides of the element (Franus et al. 2015; Frandsen 1997). The ash composition of bulk chemical ash, as determined by standard bulk chemical analysis, is as follows:

$SiO_2 + Al_2O_3 + Fe_2O_3 + CaO + MgO + Na_2O + K_2O + TiO_2 + P_2O_5 + SO_3 = 100\%$ (1)

Instead of being considered a waste, coal ash has great potential to provide much value. For instance, concrete, roads, bridges, buildings, concrete blocks, and various other concrete products manufactured using coal ash exhibit superior quality compared to those that do not incorporate coal ash (Simpson 2020). Coal ash is primarily comprised of two types, namely, bottom ash and fly ash.

During pulverized coal combustion, bottom ash is formed when coarse-grained ash particles are collected from the bottom of the boiler. The flue gases cannot carry the ashes during combustion because of their size; they impinge on furnace walls or fall into an ash hopper by openings in the furnace walls. Bottom ash has a range of colors from gray to black. It can be used as feedstock in cement manufacture, as an aggregate in construction, or as a replacement for sand and gravel in construction (Miod 2008).

During coal combustion in electric power plants, fly ash is captured by emission control equipment before it is released into the atmosphere. Fly ashes are composed of fine particle sizes ranging from 0.5 to 200 μm. The color of fly ash varies from gray to black. The colors of the ash are determined by the amount of unburned carbon present. Whiter fly ash indicates a lower carbon concentration, while darker fly ash indicates a higher carbon concentration. The main components are silica, alumina, calcium compounds, and toxic metals. These substances are used mostly in cement production, concrete mixing, and ceramic manufacturing (Twardowska and Stefaniak 2006).

Fly ashes are generally pozzolans. Pozzolan consists of siliceous and aluminous material, which in a normal temperature and moisture environment combines calcium oxide with calcium carbonate to form a cementitious compound with a number of beneficial properties (Twardowska and Stefaniak 2006).

Because of the chemistry involved in coal combustion, the composition of coal ash varies depending on the coal source and the process of combustion. Due to its composition, coal ash has a similar composition to many rocks on the surface of the Earth. It has quartz, feldspars, clays, and metal oxides derived from coal's inorganic minerals.

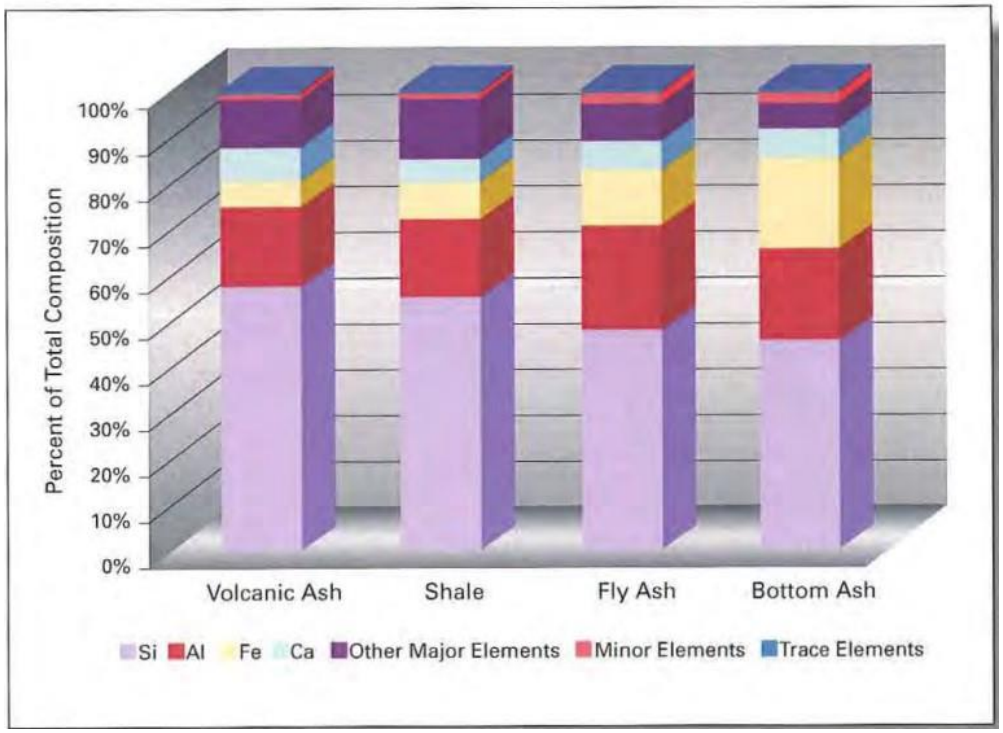

Figure 2. 1: Elemental composition of bottom ash, fly ash, shale, and volcanic ash (Jeremy DreierA., LaCaria, and Howatt 2009)

In accordance with Figure 2.1: silicon oxide, aluminum oxide, iron oxide, and calcium oxide makeup approximately 90% of the mineral components in typical fly ash, based on the average chemical composition in the example shown. In minerals, certain trace elements like arsenic, cadmium, lead, mercury, and selenium are present, but their combined concentration typically constitutes less than 1% of the overall mineral composition. In contrast, minerals contain a significantly higher proportion of minor components, comprising nearly 8% of the mineral's composition. These minor components include elements such as magnesium, potassium, sodium, titanium, and sulfur (Jeremy DreierA. et al. 2009; Kolker 2023).

2.2. Classification of Fly Ash

Coal ash is primarily composed of fly ash and bottom ash. Due to its heavier and granular nature, bottom ash has less value compared to fly ash. Typically, fly ash is classified into different size fractions according to the size requirements, thus ensuring a uniform, high-quality product (Adams,

and Ward 2015). The specific size fraction that results from this process is often used for specific markets and helps reduce residual carbon content.

Generally, fly ash is calcareous or siliceous. There are different trade names for fly ash available from ash companies, such as PozzFill, SuperPozz or Class S and Class M.

Among all classes of fly ash, Class F is the most abundant. Compared with Class C fly ash, Class F contains less lime (CaO), typically less than 15%, as well as more iron, silica, and alumina (more than 70%) (Anon 2012). In most cases, Class C fly ash is produced from coals with high levels of lime in the ash, generally over 15% but sometimes even 30%. The presence of increased CaO may lead to self-hardening properties in Class C.

2.3. Coal Fly Ash Production in South Africa

The economy of South Africa is largely dependent upon fossil fuels, and coal contributes between 91% and 93% of electricity generation (Baker et al. 2015). The country's particular dependence on coal for its power generation results in large quantities of ash being deposited on nearby land as a result of coal-fired power generation. As of the latest available data, South Africa possesses a total power generation capacity of 52.8 MW. Out of this capacity, approximately 9.2 MW, which accounts for 17.4%, is generated from renewable sources like solar PV, wind, and nuclear energy. The remaining 43.6 MW, making up approximately 82.6% of the total capacity, is powered by fossil fuels(Shikwambana, Mhangara, and Mbatha 2020). A total of 43.3 MW is derived from fossil fuels, of which 40 MW is derived from coal. A total of 18 coal-fired power plants are currently in operation in South Africa (see Figure 2.2), varying in size and capacity according to their location and utilization. Within South Africa, there are a total of 18 coal-fired power plants distributed across different provinces. Specifically, 12 of these power plants are situated in the Mpumalanga province (MP), 2 are located in the Limpopo province (LP), and 4 can be found in the Gauteng province(GP) (Hancox 2016).

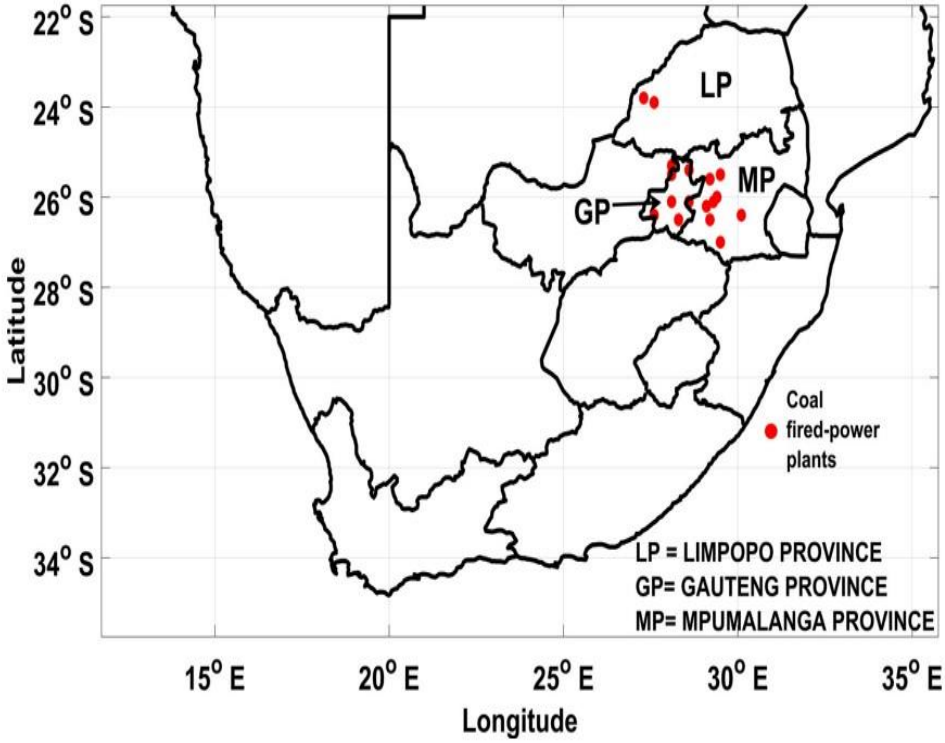

Figure 2. 2*:* Maps showing the location of coal-fired power plants in South Africa

A significant amount of coal combustion waste (CCW) is produced from fly ash through coal combustion (CFA), one of the major components. CCW is commercialized differently depending on the region. The South African industry produces over 50 million tons of CCW a year, and approximately 10% of it is reused, mostly for construction (Reynolds-Clausen and Singh 2019; Eskom 2021). The utilization rate of their resources is higher than that of countries such as the USA and Europe. In 2016, the European Coal Combustion Products Association reported that the EU produced approximately 40 million tonnes of coal combustion products and that 90% of these products were reused for construction and reclamation (Reynolds-Clausen and Singh 2019). A total of 107 million tonnes of CCW were produced in the USA in the same year, with 60% of those tonnes being processed again. By 2020, their total CCW had fallen to 40 million tonnes, while close to 58% were reprocessed (Kolker 2023; Vilakazi et al. 2022). In light of the fact that CFA is used directly as a raw material or additive

material in the building and construction sector, the building and construction sector contributes substantially to its recycling. However, managing the amount of CFA disposed of remains a major challenge.

2.3.1 Classification of REEs

Rare earth elements are commonly categorized into two main groups based on their bulk density: the "light rare earth elements" (LREEs) and the "heavy rare earth elements" (HREEs). It's worth noting that some authors expand this classification to include a third set of rare earth elements known as "middle rare earth elements" (MREEs) within their definitions(Gholz 2014; Hurst 2010). There is uncertainty regarding the precise assignment of REEs in each of these subgroups due to differences among authors regarding their interpretation of REEs in each of these subgroups. A rationale for the classification of REEs provided by the United States Geological Survey (USGS) has been incorporated into this study.

The USGS classifies REEs into only two subgroups: LREEs and HREEs. LREE relates to lanthanides with lower atomic numbers (atomic numbers 57-64) and consists of elements such as lanthanum to gadolinium. In contrast, HREE, which has lanthanides with atomic numbers from 65-71, is characterized by the presence of lanthanides of higher atomic numbers, such as terbium to lutetium. The differentiation between these two subgroups stems from the arrangement of the $4f$ electrons. In light rare earth elements (LREEs), there are unpaired electrons occupying the $4f$ orbital, whereas heavy rare earth elements (HREEs) feature pairs of electrons within the $4f$ orbital. It appears that yttrium (atomic number 39) shares a chemical composition with HREE lanthanides, so it is included as part of the HREE subgroup. However, scandium (atomic number 21), although it is included in the definition of REE, is neither a member of HREE nor a member of LREE (Gupta and Krishnamurthy 1992).

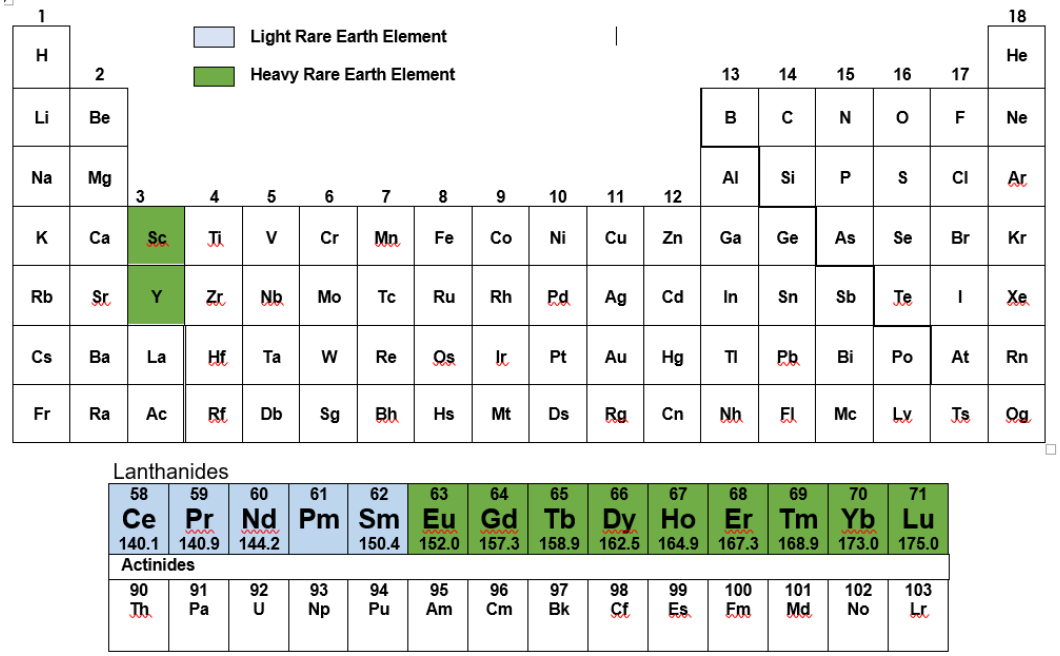

Figure 2. 3: Periodic table designation of REE and its subgroups

2.4 Chemical Properties of REEs

The REEs have a strong electropositive chemistry dominated by ionic bonds. In both chemistry and geochemistry, REEs have the most stable oxidation state of +3. In their geochemistry, REEs exhibit +2 and +4 oxidation states; however, europium and cerium are the only ones to exhibit these states in their geochemistry (Table 2.1). Because REE cations possess hard Lewis acids, they form highly labile complexes with fluoride and oxygen-containing ligands (Henderson 1984).

Table 2. 1: REE electron configuration states and trivalent ionic radiis

Atomic Number	Chemical Symbol	Elements	Electron Configuration*	Oxidation States	M^{3+} Radius/Å
21	Sc	Scanduim	[Ar]3$d^1$4s^2	+3	0.68
39	Y	Yttrium	[Kr]4$d^1$5s^2	+3	0.88
57	La	Lanthanum	[Xe]5$d^1$6s^2	+3	1.06
58	Ce	Cerium	[Xe]4f ^{1}5$d^1$6s^2	+3, +4	1.03
59	Pr	Praseodymium	[Xe]4f ^{3}6s^2	+3, +4	1.01
60	Nd	Neodymium	[Xe]4f ^{4}6s^2	+3	0.99
61	Pm	Promethium	[Xe]4f ^{5}6s^2	+3	0.98
62	Sm	Samarium	[Xe]4f ^{6}6s^2	+2, +3	0.96
63	Eu	Europium	[Xe]4f^{7}6s^2	+2, +3	0.95
64	Gd	Gadolinium	[Xe]4$f^7$5$d^1$$s^2$	+3	0.94
65	Tb	Terbium	[Xe]4f ^{9}6s^2	+3, +4	0.92
66	Dy	Dysprosium	[Xe]4f ^{10}6s^2	+3	0.91
67	Ho	Holmium	[Xe]4f ^{11}6s^2	+3	0.89
68	Er	Erbium	[Xe]4f ^{12}6s^2	+3	0.88
69	Tm	Thulium	[Xe]4f ^{13}6s^2	+3	0.87
70	Yb	Ytterbium	[Xe]4f ^{14}6s^2	+2, +3	0.86
71	Lu	Lutetium	[Xe]4f^{14}5$d^1$6s^2	+3	0.85

*Ground-state electron configuration (Huang and Bian 2010)

2.4.1. Chemical Similarity of REEs

A distinguishing characteristic of REEs is their chemical consistency among individual members of the group. Compared to other metals of the periodic table, they often exhibit a significant difference in chemical properties compared to neighboring elements in the same period (Sastri et al. 2003). As reported by several authors, this pronounced chemical similarity of REEs makes the separation and quantification of these elements more challenging because REEs display distinct chemical properties, primarily attributed to their unique electron configuration. This phenomenon is further reinforced by a phenomenon referred to as the "lanthanide contraction (Pillay 2016). A detailed description is provided of these aspects and how they enable REEs to share their characteristic chemical similarities.

2.4.1.1. Electronic arrangement of REEs

REEs are characterized by a specific electron configuration that is seen specifically in elements composing the lanthanide series of the periodic table**.** As the atomic number increases, a single electron is distributed across the periodic table**.** In conventional atomic structures, the number of valence electrons in an atom increases as this electron enters the outermost orbital. In lanthanides, the valence electrons remain relatively undisturbed, as one of the electrons exits from the inner $4f$ orbital. With the outer $5s^2$ and $5p^6$ orbitals being fully occupied, the $4f$ electrons are effectively shielded from participating in chemical bonding and interactions. This phenomenon accounts for the similar chemical behavior observed among rare earth elements (REEs) (Sastri et al. 2003).

2.4.1.2. Lanthanide Contraction

Another characteristic feature of REEs is lanthanide contraction, which is caused by the unusual electron configuration. Lanthanide contraction occurs as the atomic number of REEs increases, resulting in a progressive decrease in the ionic radius. When the nuclear charge increases with atomic

number, there is insufficient shielding between one $4f$ electron and another (Editor 2013). This causes each $4f$ electron to be drawn closer to the nucleus, causing the ion to shrink in size as well as the size of the $4f$ orbital (figure 2.4).

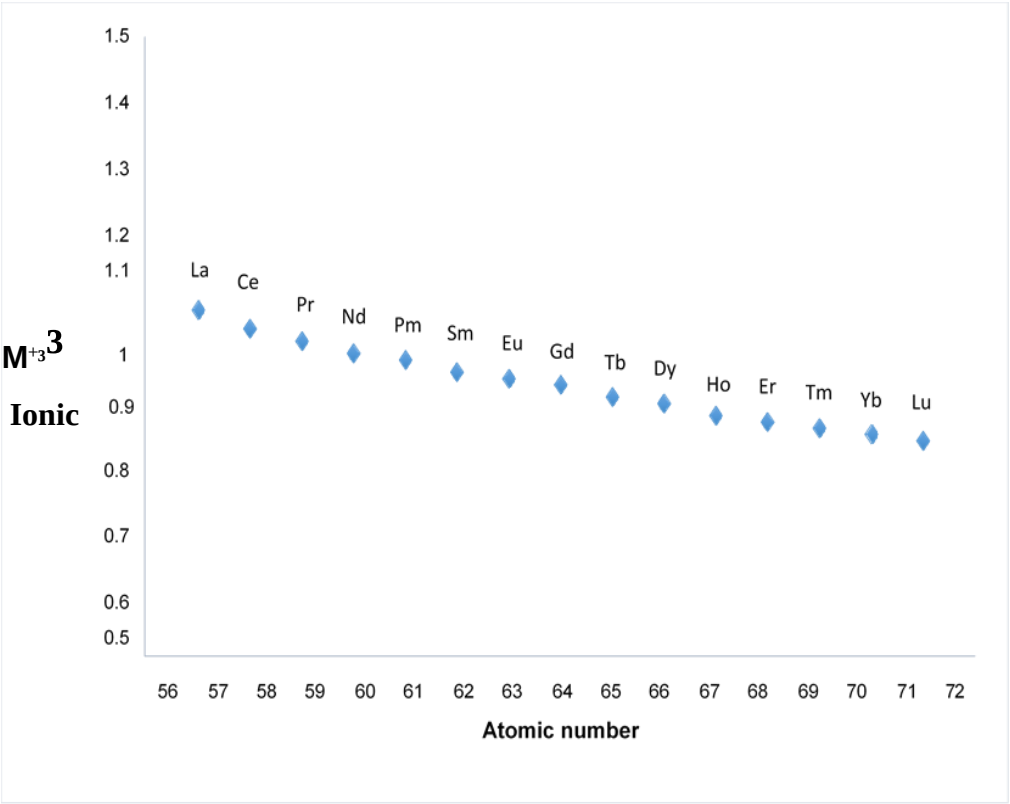

Figure 2. 4: Lanthanide contraction; decrease in ionic radii with an increase in atomic number

2.5. Occurrence of REEs

In the field of geochemistry, rare earth elements (REEs) are classified as "lithophile" elements because they tend to associate with oxygen-containing minerals like silicates, phosphates, and carbonates. These elements have an affinity for bonding with oxygen and are often found in the Earth's crust within these types of mineral compounds (Adams., and Ward 2015). As a whole, these elements occur in mineral assemblages, not in pure metals or separate elements. As a result of their similar ionic radii, trivalent REE ions are capable of replacing each other in host minerals. The odd-even effect (Oddo-Harkins rule) is clearly evident in REEs found in the Earth's crust, where even atomic number elements are concentrated more than odd atomic number elements (Sastri et al. 2003). Consequently, it is well known that REEs with neighboring positions on the periodic table have unequal concentrations in geological materials. In addition, geological materials have higher levels of LREEs than HREEs (Adams, and Ward 2015).

Currently, approximately 200 minerals have been identified to contain REEs. While REEs occur in numerous minerals, they are typically present in low concentrations that make them economically viable to mine and, as a result, are difficult to obtain. Several types of rare earth elements (REEs) are economically significant, and these include bastnäsite, monazite, xenotime, and ion adsorption clays. These minerals are valuable sources of REEs, which are essential in various technological and industrial applications (Gupta and Krishnamurthy 1992).

2.5.1. Basenäsite

Basenäsite is a mineral that belongs to the carbonate class. Its chemical formula is $Na_3Ca(CO_3)_2$. Basenäsite is typically found in alkalic pegmatites and nepheline syenites. It was first discovered in the late 19th century in Greenland and was named after the type locality at Basenäset, Sweden. Basenäsite is an important source of rare earth elements (REEs), such as cerium, lanthanum, and neodymium (Gupta and Krishnamurthy 1992).

One of the most interesting things about basenäsite is its potential use in the production of rare earth metals. Rare earth metals are essential components in many modern technologies, including smartphones, wind turbines, and electric cars. Basenäsite contains high levels of rare earth metals, making it a valuable resource for researchers and manufacturers.

In addition to its potential use in the production of rare earth metals, basenäsite also has a number of other applications. It can be used as a gemstone and is sometimes cut into cabochons for use in jewelry. It is also used in the production of some types of ceramics and glass.

2.5.2. Monazite

The minerals monazite, REE, and $ThPO_4$ are phosphate minerals. Its main constituents are lithium, rhenium, and ethidium, with a 55-60 wt.% REE content. Although monazite contains a high proportion of rare earth elements, the high thorium content of the mineral and associated radioactive waste handling problems have caused it to be discontinued for mining (Gupta and Krishnamurthy 1992).

The largest deposits of monazite are found in Australia, India, and Brazil. Other countries that produce monazite include the United States, Malaysia, and South Africa. Monazite is typically extracted from beach sands or from hard rock deposits using a combination of physical and chemical separation techniques.

The mineral is an important source of rare earth elements, which are used in a variety of high-tech applications, including magnets, catalytic converters, and rechargeable batteries. Monazite is also a source of thorium, a radioactive element that can be used as a fuel in nuclear reactors.

2.5.3. Xenotime

Xenotime is a rare earth phosphate mineral primarily composed of yttrium, phosphorus, and oxygen. It is an important source of yttrium and can also contain other rare earth elements, making it valuable for various industrial applications. It was first discovered in 1824 in Sweden and was named after the Greek words "xenos" and "time," which mean "strange" and "honor,", respectively. Xenotime has a unique crystal structure that makes it an important mineral for a variety of applications. It is commonly used as a source of yttrium and other rare earth elements for use in electronic devices, such as flat-panel displays, LEDs, and magnets. Its high yttrium content also makes it useful in nuclear reactors.

Xenotime is typically found in igneous rocks and pegmatites, and it can also be found in alluvial deposits. It is often associated with other rare earth minerals, such as monazite and bastnäsite. Although xenotime is a valuable mineral, it is not commonly mined due to its rarity and the difficulty of extracting rare earth elements. However, there has been renewed interest in xenotime mining in recent years due to the increasing demand for rare earth elements and the geopolitical concerns surrounding their supply.

In conclusion, xenotime is a unique and important mineral that has a variety of applications in modern technology. Its rarity and difficulty of extraction make it a valuable resource, and it is likely to play an increasingly important role in the future as demand for rare earth elements continues to grow (Gupta and Krishnamurthy 1992).

2.6. Significance of REEs

It is important to understand the significance of REEs in technology. As inputs to manufacturing advanced technologies, they are of vital importance for the development of modern technology. There is a wider variety of consumer products available from rare earth elements than any other elemental grouping. A consumer electronic product is something we use every day, such as a mobile phone, television, laptop, or computer (Du and Graedel 2011). Many of the applications of REEs are due to their unique magnetic, optical, luminescent, and catalytic properties. In addition to these applications, REEs have been at the forefront of sustainable technological inventions, which have enhanced their commercial worth (Bartlett 2011).

Additionally, the COVID-19 pandemic has forced the whole world to rapidly adapt to the use of different technological devices. The use of REEs in green technologies has been expanding recently, for example, for phosphorescent lighting and wind turbine generators, as well as for producing lightweight permanent magnets and high-capacity battery packs for electric and hybrid vehicles (Bartlett 2011). Additionally, the COVID-19 pandemic has forced the whole world to rapidly adapt to the use of different technological devices. Additionally, REEs have gained economic significance as a result of increased environmental awareness and the subsequent global transition toward a green economy. It is anticipated that REE will experience an increase in demand due to its use in green technologies in the near future, which may result in a shortage of supply (Robert et al.2012).

2.7. Uses and Application of REEs

REEs are used in many industrial and technological applications due to their unusual physical and chemical properties. As a result of their similar chemical nature, REEs have numerous uses that are related or complementary; therefore, it is more convenient to describe their applications by applications rather than by element. In general, the lighter rare earth elements (LREEs) and yttrium are typically more affordable, more

abundant, and have a broader range of applications compared to the heavier rare earth elements (HREEs). A few highly specialized, highly expensive REEs, such as lutetium and holmium, are commonly used in high-tech applications.

Raw rare earth elements (REEs) are primarily utilized by the glass industry for various purposes, including glass polishing and as additives to impart specific colors and unique optical properties to glass products. The optical properties of REEs make them valuable in achieving desired visual effects and functionalities in glass manufacturing (Paper 1802). A high level of precision polishing is needed for flat panel display screens, which are made of cerium oxide. Decolorizing glass is also done with cerium. The optic glass becomes more refractive with the addition of lutetium and lanthanum. A high refractive index is essential for immersion lithography, which uses lutetium instead of lanthanum, which is commonly used in cameras. Glass is colored with erbium, holmium, neodymium, praseodymium, ytterbium, and yttrium and provides glare-reduction and filtering properties. Optical fibers commonly contain europium as a doping agent (Schramm 2016).

Several REEs are also used as catalysts, including lanthanum catalysts for petroleum refinement and cerium catalysts for automotive catalytic converters (Tuan et al. 2019). Rare earth element (REE)--riched catalysts play a crucial role in petroleum refineries by breaking down heavy hydrocarbon molecules into smaller molecules. This process allows refineries to increase their oil processing capacity and efficiency, as heavy hydrocarbons are converted into lighter and more valuable products, such as gasoline, diesel fuel, and other refined petroleum products. Carbon monoxide emissions are reduced using catalysts made of neodymium, praseodymium, and yttrium in automotive catalytic converters.

As permanent magnets made from alloys of rare earth elements become increasingly popular, they are generally used where space and weight are limited. Neodymium-iron-boron magnets are the strongest magnets known. The use of electric motors extends beyond hard drives and cell phones to

hybrid vehicles, windmills, and aircraft actuators (Du and Graedel 2011). These magnets contain less dysprosium, gadolinium, and praseodymium than they used previously.

As an important part of permanent magnets, dysprosium can replace a small portion of neodymium in high-temperature applications, such as electric motors for hybrid cars and wind turbines. When heat stress is an issue, samarium-cobalt magnets are used in place of neodymium magnets since they have a greater heat tolerance. Nickel-metal hydride batteries contain anodes made from lanthanum alloys (Bartlett 2011).

Battery alloys containing cerium, neodymium, praseodymium, and samarium are used in many rechargeable consumer products and hybrid vehicles. A gadolinium phosphor is used in medical imaging and X-rays, whereas ceramic pigment contains yttrium, lanthanum, cerium, neodymium, and praseodymium as ingredients. The use of rare-earth elements is also widespread in manufacturing synthetic gems, laser crystals, microwaves, superconductors, sensors, nuclear control rods, cryocoolers, and fertilizers (Tuan et al. 2019).

2.8. Analytical Techniques used for determination of REEs

This section reviews techniques that are commonly used to identify potential associations between REEs, coal, and combustion products. As the spectrometric determination of REEs currently dominates research, this review has mainly discussed the spectrometric determination of these elements. This study utilized a range of techniques for analysis. Among these, X-ray diffraction (XRD), X-ray fluorescence (XRF), scanning electron microscopy (SEM), and inductively coupled plasma–mass spectrometry/optical emission spectrometry (ICP–MS/OES) were employed to gather data and information.

2.8.1. X-ray fluorescence

X-ray fluorescence spectrometry (XRF) involves irradiating samples with primary X-rays to stimulate the emission of secondary/fluorescent X-rays. By measuring X-rays, one can identify the elemental constituents of a sample by quantifying their energy using energy dispersive (EDXRF) or wavelength dispersive (WDXRF) (Robinson et al.1986).

XRF provides many valuable analytical capabilities, including the ability to analyse samples directly and detect multiple elements. Due to these combined aspects, it is possible to quickly determine the presence of REEs by performing an analysis without sample preparation, as well as quantifying all REEs in a single analysis. Although this technique offers a variety of benefits, it is severely restricted by spectral interference. Spectral interference is caused by the emission of matrix elements that overlap the X-ray energies and/or lines that are used to detect REEs (Zawisza et al. 2011).

The low detection limits of XRF for measuring REEs are further indicators of the limitations of the method. For geological samples, these values are in the g-1 (ppm) range, which is not satisfactory for finding REEs, especially HREEs, which have ng g-1 (ppb) concentrations (Zawisza et al. 2011).

2.8.2. X-ray diffraction (XRD)

X-ray diffraction (XRD) is a widely used analytical technique in materials science and solid-state physics. It is based on the principle of analysing the scattering of X-rays by crystalline materials to determine their atomic and molecular structure (Bunaciu et al. 2015).

The principle behind XRD is that when a beam of X-rays is incident on a crystalline material, the X-rays are scattered in different directions by the atoms in the crystal lattice. These scattered X-rays interfere with each other, resulting in a diffraction pattern that can be recorded and analysed. The diffraction pattern is a series of bright spots, known as diffraction peaks,

which correspond to the different planes of atoms in the crystal lattice. By measuring the angles and intensities of these diffraction peaks, information about the crystal structure, such as lattice parameters, unit cell dimensions, and atomic positions, can be obtained (Bunaciu et al. 2015) JoVE, Cambridge 2023).

X-ray diffraction (XRD) is a versatile analytical technique employed in various fields such as materials science, geology, chemistry, and pharmaceuticals. It serves multiple purposes, including the identification and characterization of crystalline materials, determination of crystal structures, measurement of crystallographic parameters, and the investigation of phase transformations and crystal defects. Its widespread utility makes it a valuable tool for understanding the atomic and molecular arrangements in a variety of substances (Bunaciu et al. 2015).

In XRD experiments, a sample is usually prepared as a fine powder or a single crystal, depending on the nature of the material being studied. The sample is then placed in the X-ray beam, and a detector is used to measure the intensity of the scattered X-rays at different angles.

XRD instruments can be equipped with different types of X-ray sources, such as rotating anode generators or sealed X-ray tubes, which produce X-rays with different wavelengths. The choice of X-ray source depends on the specific requirements of the experiment and the type of material being studied (JoVE, Cambridge 2023).

In conclusion, XRD is a powerful technique for analysing the atomic and molecular structure of crystalline materials. It has widespread applications in materials science and solid-state physics, providing valuable insights into the properties and behavior of various materials.

2.8.3. Inductively Coupled Plasma–Mass Spectrometry

ICP–OES and ICP–MS are analytical techniques for determining elements by inductively coupled plasmas-optical emission and mass spectrometry, respectively.

As a traditional method of ICP-MS, peristaltic pumps are used to introduce sample solutions into the instrument, followed by pneumatic nebulizers, where argon gas is used to turn these solutions into aerosols. The large droplets in the sample aerosol are discarded into a drain once they reach the spray chamber, allowing only the fine samples to enter the ICP torch (Balaram 1996).

The ICP torch has concentric quartz tubes that are surrounded by a radio frequency coil that provides argon gas flow. By combining RF coils with high-voltage sparks, this intense magnetic field generates high-temperature plasma after ionizing argon gas (10 000 K)(Balaram 1996).

In addition to dissolving, vaporizing, converting into free atoms, and finally ionizing the aerosol, it undergoes several other processes when heated plasma is introduced. In mass spectrometry, as ions exit the plasma, they are directed towards the mass spectrometer for analysis. The ions generated by the plasma at atmospheric pressure (typically around 760 torr) are then transported through a series of vacuum stages to reach higher vacuums and lower pressures, often as low as 10^-6 torr. This reduction in pressure is necessary for the proper functioning of the mass spectrometer, as it enables the separation and analysis of ions based on their mass-to-charge ratios with minimal interference from collisions with gas molecules. An interface cone, which is made of nickel or platinum, steps down pressure by maintaining a low vacuum (10-3 torr) using two cones known as the sampler and skimmer. In a mass spectrometer, sample ions enter the vacuum chamber through small orifices (0.6 - 1.2 mm) (Pillay 2016).

The ion-focusing lenses transfer the ions electrostatically to the mass analyser as soon as they enter the vacuum chamber. The applied

electrostatic potential attracts analyte ions to a mass analyser by applying a charge opposite theirs. A mass spectrometer chamber's electrostatic potential prevents both photons and neutral species from entering the chamber, in addition to repelling oppositely charged ions (Balaram 1996).

An ICP–MS with a quadrupole mass analyser is the standard configuration available on the market. In standard configurations, quadrupoles act as mass filters that allow only ions with specific mass-to-charge ratios (m/z) to enter detectors. A series of cylindrical parallel rods form the instrument, whereby varying voltages and radio frequencies allow ions of a certain mass to travel along the rods and reach the detector at a stable trajectory (Balaram 1996).

A quadrupole mass analyser converts ions that emerge from a quadrupole to measurable signals with the help of an electron multiplier detector. Electrons are released when ions interact with charged surfaces (called dynodes). The released electrons are then struck by another dynode, causing a multiplication of electrons (Pillay 2016).

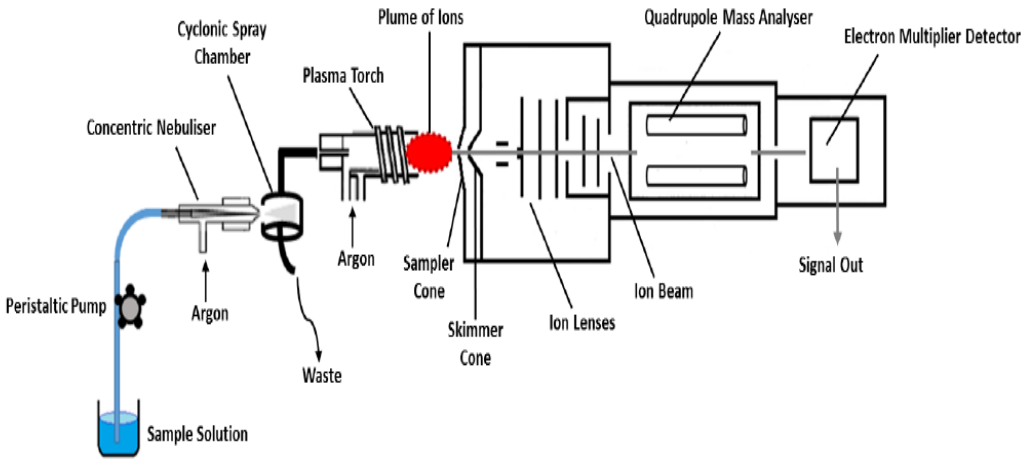

Figure 2. 5: Schematic diagram of ICP–MS instrumentation (Pillay 2016).

2.8.4. Inductively coupled plasma–optical emission spectrometry (ICP–OES)

As illustrated by ICP-OES (inductively coupled plasma–optical emission spectrometry), ions and atoms are quantified by measuring the electromagnetic radiation they emit. ICP-OES offers several significant analytical advantages, including high specificity, a broad linear dynamic range, and excellent accuracy and precision. These qualities make it a powerful analytical technique for the precise determination of elemental composition in various samples. As a result, it can be used to detect the amount of constituents in samples based on their elemental content.

There are several advantages to ICP-OES over other excitation sources, including its ability to efficiently and reproducibly vaporize, atomize, excite and ionize elements within a wide range of sample matrices, making it a very powerful analytical tool. The observation zones of the ICP-OES are situated at exceptionally high temperatures, typically in the range of 6000-8000 Kelvin (K). This temperature range significantly exceeds the maximum temperatures achievable with flames or furnaces, which typically reach up to 3300 K. This capability is primarily attributed to the ICP's extraordinarily high temperature, which is a key factor contributing to its effectiveness in analytical applications. In addition to the excitation of refractory elements, ICPs are less susceptible to matrix interferences because of their high temperatures (Hou et al. 2017).

Samples are introduced into the central channel of an ICP-OES through an introduction system in the form of a gas, vapor, or aerosol. This may involve fine droplets or solid particles, depending on the nature of the sample and the specific analytical requirements. In general, ideal sample introduction systems should have the ability to handle samples of all phases (solid, liquid, or gas), tolerate complex matrixes, and be capable of analysing very small amounts of samples (<1 mL or <50 mg) with high stability and reproducibility, simplicity, low cost, and high transport efficiency (Hou et al. 2017).

ICP OES usually employs nebulizers to introduce solution samples. By vaporizing a sample with a nebulizer, it is transported to the plasma. Aerosols in the context of ICP (Inductively Coupled Plasma) typically consist of extremely fine droplets, usually around 8 micrometers (µm) in diameter, which are suitable for injection into the plasma. Traditionally, ICP analysis involves the use of spray chambers located between the nebulizer and the torch. These chambers serve to remove larger droplets from the aerosols and help dampen any potential pulses that might occur during nebulization. This process is beneficial as it reduces the amount of liquid introduced into the plasma, thereby enhancing stability, particularly when working with organic solvents (Pillay 2016). Refer to Figure 2.6 for illustration.

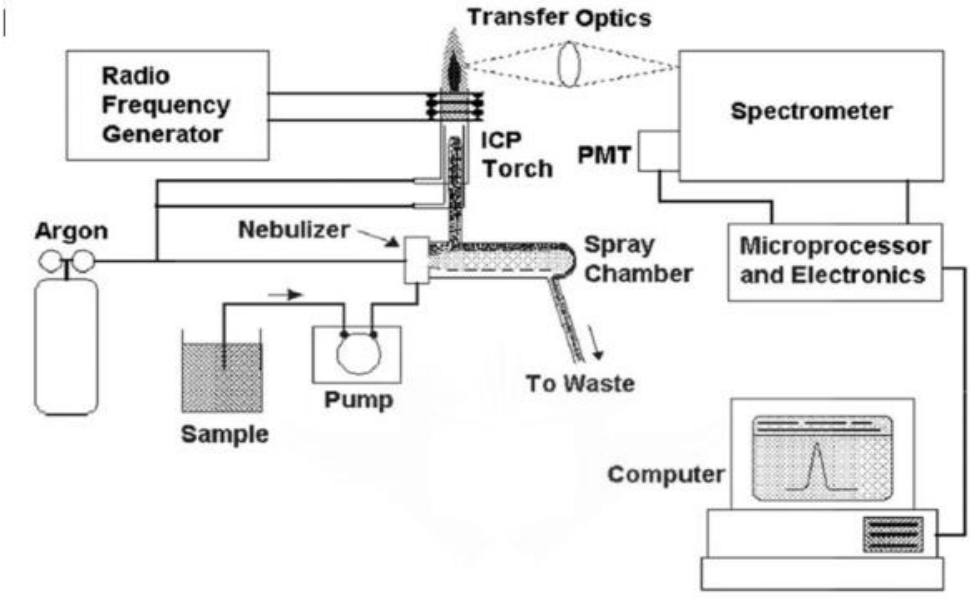

Figure 2. 6: Schematic diagram of ICP– OES instrumentation (Pillay 2016).

2.8.5. Comparison between ICP–MS and ICP–OES

There are a variety of analytical techniques available for determining elemental compositions, including inductively coupled plasma–optical emission spectrometry (ICP–OES) and inductively coupled plasma–mass spectrometry (ICP–MS). In recent years, there has been a debate about the attractiveness of ICP–OES as an analytical technique, leading many analysts to consider whether it might be more advantageous to invest in ICP–OES instrumentation rather than continuing with traditional atomic absorption spectroscopy (AAS). This discussion stems from the enhanced capabilities and broader analytical range that ICP-OES offers compared to AAS. The choice between these techniques would depend on specific analytical needs and budget considerations (Tyler and Group n.d.). ICP-OES was introduced as a new, more expensive technique, and inductively coupled plasma–mass spectrometry has gained popularity. Figure and Figure show the typical components and layout of an ICP–MS and OES, respectively.

The same sample introduction system and plasma are used in both ICP–OES and ICP–MS. Using ICP-OES, it is possible to view and measure optical spectra sequentially or simultaneously depending on the situation, typically ranging between 165 and 800 nm (Tyler and Group n.d.). For large numbers of elements, simultaneous ICP-OES can be faster but more expensive. This can be determined by the amount of concentration or the number of elements needed. With ICP–OES spectrometers capable of reaching 120 nm, Cl can now be determined with subppm detection limits at the primary wavelength of 134.664 nm (Yu and Anashkin 2019).

In ICP-MS, the plasma ions are extracted by sampling them and removing them from a sampler and skimmer interface. This configuration enables the pressure differential to be reduced from atmospheric pressure to a final

pressure of between 10^{-5} Torr and 10^{-7} Torr. By using ion optics, the ions are processed by eliminating neutral species and light, and a photon stops the light after they have passed through the interface. A mass filter collects the ions after they pass through it. The selected ions usually first pass through a quadrupole before reaching the detector (Hou et al. 2017).

Due to its ability to detect multiple elements over a wide range of concentrations, ICP-OES is often used to determine REEs. Samples usually contain much lower levels of REEs than this technique has the capability of detecting, and some matrix effects may be caused by other constituents, including organic compounds and inorganic salts (Yu and Anashkin 2019).

One of the most powerful techniques for determining lanthanides is ICP–MS. The technique contains a high degree of sensitivity, has a wide dynamic linear range, is capable of multielement analysis, and has the ability to measure isotopes. When compared with ICP–OES, ICP–MS will be able to produce simpler spectra and lower detection limits, making it possible to determine REEs in soils without having to separate the matrix. The problem of spectral interference, however, remains an ICP–MS analysis challenge. The most common way to resolve ICP–MS interferences is through a combination of a high degree of resolution, reaction/colliding cells, and separation. For most samples, it is sufficient to make a mathematical correction to resolve the interference issue (Drobne et al. 2018).

To analyse solid samples using ICP–OES, and ICP–MS, standard reference solutions are needed. As a consequence, trace element assessments are concerned with the preparation of these solutions. Depending on the desired concentration, standard solutions or metal salts of high purity need to be dissolved or diluted with appropriate reagents. To make the instrument

respond to standards and samples in the same way, it is essential to match the standard matrix with the sample matrix (Derkach and Baula 2017). For example, if nitric acid is present in the sample at 1%, then nitric acid should be present in the standard at the same concentration.

Based on the sample's chemical and physical properties, the type of acid or a combination of acids to use, along with the recommended amount of heat and pressure applied, will determine the success of digestion (Derkach and Baula 2017).

2.9. Previous Studies done by other researchers

January 2017. The Department of Energy, National Energy Technology Laboratory (DOE/NET) conducted a practical investigation based on the economic recovery of rare earth elements from coal and coal byproducts such as fly ash, coal refuse, and aqueous effluents. This assessment was conducted several times under various conditions to evaluate REEs connected with a large amount of coal from basins in the U.S. Almost 30,000 isolated REEs were analyzed from approximately 18,000 samples that were collected from different sources. A preliminary reserve base was established from two key coal production regions in the U.S. This was based on both observations from a literature survey and a practical investigation of testing samples from a mining operation. According to the study, the global REE market demand will remain on the order of 100,000 tonnes annually, with the U.S.'s current two regions alone holding reserves of almost millions of tonnes.

According to this finding, recovering and separating REEs that are physically and chemically involved will pose challenges in the distribution of REEs in coal and coal byproducts, which will require more information and advanced techniques to achieve this goal. The limited data collected in the

course of this assessment were used to identify promising methods that can be applied to various source streams in the coal value chain to concentrate REEs.

Taggart et al., (2018) studied the effects of roasting additives and leaching parameters on the extraction of REEs from coal fly ash. The aim of this research was to determine the key parameters and reagents used to control REE extraction and to test techniques used to improve the extraction of REEs from fly ash. Different coal ash samples from different coal power stations in the U.S., such as the Powder River Basins, Illinois, and Appalachian, were roasted using different chemical additives (Na_2O_2, NaOH, CaO, Na_2CO_3, $CaSO_3$, $(NH_4)_2SO_4$). Various parameters were investigated, including additives, roasting temperature, and leaching pH. Studies have also been performed to determine the effects of additives, ash ratios, and roasting temperatures on the extraction of REEs. It was found that over >90% of the REE content was determined by the sodium hydroxide (NaOH) roasting method, which is equivalent to the Na_2O_2 sintering method recommended by the USGS. The obtained results of the total REE content from the additive test recovered <50% and the contributing factor for low recovery may have been a sintering temperature of 450°C, which was below the melting point of those reagents. It was found that REE recovery was not significantly inhibited by decreasing the NaOH/ash ratio while increasing the leachate pH led to a sharp decline. The leaching H^+ molarity found between REE extractions shows a strong positive correlation. Despite the roasting agent and additive ash ratio in the Powder River Basin ash sample, a recovery of $\sim$ 100% was achieved. A single acid leaching treatment was found to be sufficient for the recovery of REEs from more soluble Powder River Basin ashes.

Peramaki., (2006) studied method development for the determination and recovery of rare earth elements from industrial fly ash. Rare earth element concentrations were determined from a mixture of peat and biomass fuel fly ash collected from Finnish power plants. Different methods were used for pretreatment, such as microwave-assisted acid digestions and ultrasound methods for the digestion of fly ash samples. The reliability of inductively coupled plasma optical emission spectroscopy (ICP–OES) was determined by comparing it with inductively coupled plasma–mass spectrometry (ICP–MS) under the same measurement conditions and using standard reference materials, synthetic samples, and standard addition methods to evaluate the reliability of the analysis. From this study, it was found that most fly ash samples are enriched with rare earth element concentrations compared with other earth crust elements. The concentration of REEs from other ashes was found to be approximately 560 mg kg^{-1}, which was slightly high.

The dissolution leaching procedure of dilute sulfuric acid was developed in this experiment to dissolve rare earth elements from fly ash samples collected from a specific area. Approximately 70% of REEs from fly ash samples were dissolved by sulfuric acid leachate optimization. Liquid–liquid extraction and oxalate precipitation were used in this investigation to recover REEs by a sulfuric acid leaching procedure. It was shown that bis(2-ethylhexyl)phosphoric acid (D2EHPA), which can concentrate rare elements with liquid–liquid extraction methods, was able to concentrate rare elements quantitatively but nonselectively when conditions were optimal for oxalate precipitation. Furthermore, it was shown that bis(2-ethylhexyl)phosphoric acid (D2EHPA) could simultaneously concentrate rare elements. In conclusion, it was stated that it is possible to achieve the recovery of light and heavy rare earth elements by the leaching process and optimization parameters.

Wagner and Matiane (2018b) conducted a study on a variety of coal and coal ash samples from the Main Karoo Basin of South Africa to test for rare earth elements. The purpose of the study was to determine the levels of REY+Sc produced by South African coal feed stations and their associated ash products (eight samples) based on REY+Sc produced from coal feed stations and their associated ash products. Various advanced techniques include inductively coupled plasma–mass spectrometry (ICP–MS), X-ray diffraction (XRD), instrumental neutron activation analysis (INAA) and petrography Malvern particle size analysis. In their finding, they determined that H^- and M^- types of enrichment with REY were determined, and the total concentration of REY was found to range from 95 to 149 ppm in coal samples, which is higher than the upper crustal average, as well as the global hard coal ash average, but lower than REY-rich coal ash records worldwide.

Mketo et al., (2014) investigated the extraction of total sulfur from coal samples using microwave-assisted acid followed by ICP–OES analysis. Certified reference materials (SARM20) were used to optimize parameters that affect microwave-assisted acid extraction, such as microwave temperature, extraction concentration, extraction time, mass of coal weighed, and volume of acid used HNO_3:H_2O, which is necessary to retain the total quantitative recovery of sulfur. The optimal conditions for the extraction procedure were determined to be as follows: a microwave temperature of 180 °C, an extraction time of 5 minutes, concentrations of 3 mol/L for both HNO_3 and H_2O_2, 0.05 grams of coal, and a volume ratio of HNO_3 to H_2O_2 at 2:1. These specific parameters were found to yield the best results for the extraction process. A total of three coal-certified reference materials (SARM 18, 19, 20) were analysed to test the accuracy of the microwave-assisted acid extraction method. The results indicated that

83%- 102% of the coal-certified reference materials were efficiently recovered.

Mketo et al., (2016) conducted an investigation of trace element extraction from coal samples with microwave-assisted digestion and diluted hydrogen peroxide followed by mass spectrometry inductively coupled plasma. With the help of microwave-aided digestion and using dilute hydrogen peroxide (H2O2) as the digestion medium, inductively coupled plasma–mass spectrometry (ICP–MS) is used to rapidly extract trace elements from coal samples. An acid waste reduction method using H_2O_2 diluted with water has been used in analytical laboratories to reduce acid waste emissions. Trace elements were extracted more efficiently with dilute nitric acid after H_2O_2 digestion. Through the use of coal-certified reference materials (SARM 20) in the analysis of the target, a set of key parameters related to extraction efficiency was investigated. In this study, the efficiency of the digestion process and the recovery of trace elements were significantly enhanced when the following conditions were employed in combination: a concentration of 7 mol/L for HNO_3, a temperature of 200°C, a coal sample amount of 0.1 grams, and a digestion time of 10 minutes. This set of parameters led to improved results in terms of digestion efficiency and the quantitative recovery of trace elements.

It was found that all three certified reference materials (SARM 18, 19 & 20) showed close agreement between the obtained measurements and those certified by the suppliers for the majority of the trace elements investigated. In the extraction process, elements such as Sc, V, Cr, Y, and La exhibit moderate extraction efficiency, typically ranging between 70% and 80%. However, elements like Ti and Hf have relatively poor extraction accuracy, typically falling within the range of 10% to 50%. These differences in extraction efficiency reflect the varying behavior of elements during the

analytical procedure. For the analysis of trace elements in three South African coal samples, the microwave-assisted digestion method was found to be comparable with literature reviews.

Smoli et al.,(2016) performed a study of the determination of rare earth elements in combustion ashes from selected Polish coal mines by wavelength dispersive X-ray fluorescence spectrometry. This study was conducted with the aim of devising and validating a method that could identify the presence of 16 rare earth elements (REEs) in 169 samples of coal combustion ash in ten Polish coal mines in addition to developing a technique based on wavelength dispersive X-ray fluorescence (WDXRF). According to the results, the variability of REEs in coal ashes is quite diversified in terms of levels, ranges, and distribution. XRF techniques appear to be possible and simple since the sample does not need to undergo complex preparation. It also offers an opportunity to determine trace and main components simultaneously in a short period of time. However, there are some encountered difficulties that must be considered before WDXRF techniques can be successfully applied. In particular, matrix effects (absorption and enhancement) and peak overlapping are of great importance to consider when working with WDXRF.

Considering these analytical difficulties, it is unreasonable to assume that WDXRF will be able to achieve better or even equal limits of quantification, which are available using techniques such as ICP–OES, ICP–MS, and NAA. While WDXRF is not as time-consuming or as expensive as other methods, it is much quicker than other methods, and high-quality samples can be prepared with no time-consuming preparation process. Furthermore, the measurement time is not too long, usually a few minutes. As a result of the simplicity of the sample preparation, there is less likelihood of contaminating or losing the analyte in the process. Hence, WDXRF techniques may not be

able to determine the concentration of all REEs in solid materials with high accuracy and precision. With its time- and cost-effective functionality, it could be widely applied to evaluate the level of REE concentration in a wide range of solid materials.

Savic (2008) performed a study on the optimization of the microwave-assisted acid digestion method for the determination of trace elements in coal and coal fly ash. In the findings, they concluded that XRF techniques are very good since the preparation of the sample is fast and easy, and it is capable of doing multiple elements analyses at the same time, it is also capable of showing a high precision percentage and reproducibility in a short measure time. However, due to the level of trace element concentration in ash samples compared to coal samples, XRF analysis is more suitable for ash samples than for parent coal. During this study, it was observed that the presence of coal matrix elements can lead to the absorption or enhancement of secondary X-rays. This phenomenon occurs as a consequence of the absorption or enhancement of primary X-rays. The interaction of coal matrix elements with X-rays can influence the analytical results and should be taken into consideration in the study's findings.

Atomic emission spectroscopy (AES) is the most suitable method for determining the level of trace elements in coal in regard to mining and processing. These techniques analyse the sample by exciting the samples to produce visible line spectra characterized by present elements. To determine the concentration of present elements, the line intensities of each element obtained are compared to the line spectra of known standards. The inductively coupled plasma atomic emission spectroscopy (ICP–OES) method has been used quantitatively to determine trace elements more than other techniques. ICP–OES techniques use high-temperature plasm generated by argon gas to excite the sample on an induction coil tube.

ICP-OES has multiple advantages compared with other techniques, such as the ability to quantify and identify multiple elements in a very short period of time, and it requires a very small amount of sample. Elements that are not well detected by ICP-OES are inert gases such as argon. Various wavelengths with different sensitivities are shown for the determination of one element. Inductively coupled plasma atomic emission spectroscopy is suitable for the detection of all major elements with concentrations from ultratrace levels. This is because it has low detection limits, which can detect from a typical range of 1−100 g/L for most elements. Compared with other atomic spectral methods, ICP techniques have better comparable detection limits. With plasma excitation, more elements can be detected at 10 ppb or less than with any other emission and absorption methods. For trace elements, ICP analysis has several disadvantages that should be considered. When conducting ICP measurements, different types of interference may occur, especially at low concentrations of the analytes, and these interferences can be spectral, physical, chemical, and biological.

CHAPTER 3: METHODOLOGY AND EXPERIMENTAL

The objective of this section is to provide a comprehensive discussion of the materials and methods employed to address this study's specified aim and objectives. It includes detailed descriptions of the methods, procedures, and tools utilized for data collection. This section serves as a crucial foundation for understanding how the study was conducted and how the data was gathered. A flowchart illustrating the research methodologies applied for this project is shown in Figure 3.1.

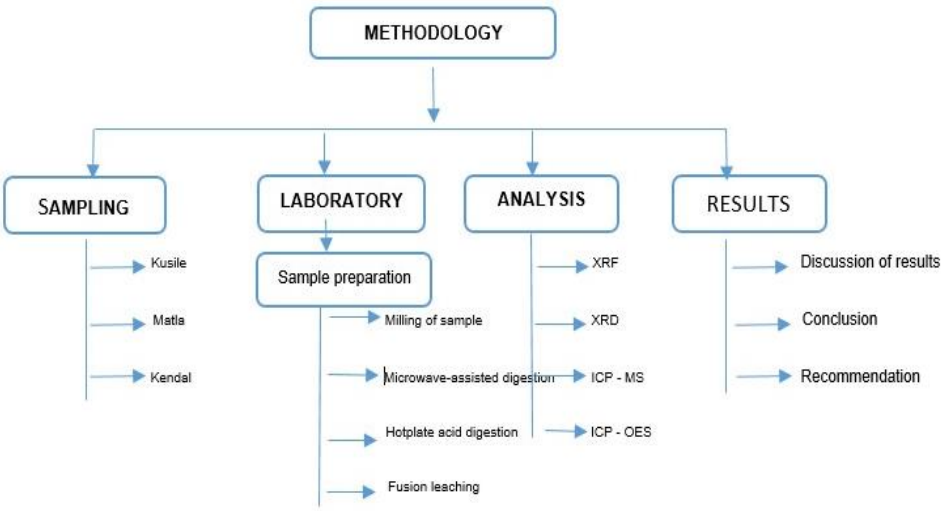

Figure 3. 1: Research methodology summarized in the flow chart

3.1. Sample Collection

Three coal fly ash samples were collected from various power stations: Kusile, Malta, and Kandel. The three coal power stations are in Highveld Coalfield which is located in the south of the Witbank Coalfield. The Coalfield spans approximately 95km in width, extending from Nigel in the west to Davel in the east. In a north-south direction, it is around 90km in length, stretching from just north of Kriel to beyond Standerton in the south. The total area covered by the Coalfield is approximately 7,000 km^2. Following the Witbank Coalfield, the Highveld Coalfield is the second-largest coal-producing region in South Africa. In both the Witbank and Highveld coalfields, five distinct coal seams can be identified. These seams are labeled from 1 to 5, starting from the bottom and progressing upward. Each seam is part of a depositional sequence primarily consisting of sandstone, and gritstone, along with interbeds of finer siltstone and mudstone(Justin and Muaka 2013).

A sample weighing 20 kg was collected from the Kusile power station, and it was categorized as fly ash, with classifications of both Class N and Class S. The Malta and Kendal power stations provided 20 and 5 kg, respectively. Malta ash showed an identity of classified and unclassified materials, while the ash from the Kendal power station was identified as Duraposs. The collected samples were packaged in plastic containers and plastic bags respectively. Table 3.1 shows the identification of the ash samples. All the samples were milled to pass 85% of 75 m before they could be prepared for analysis.

Table 3. 1: Ash sample identification

Station	Sample ID	Ash Class
Kusile	Quartz	Class C
	Magnetite	Class F
	Mullite	Class F
Malta	Magnetite	Class N
Kendal	Durapozz	Class C

3.2. Certified Reference Materials (CRMs)

Three certified reference materials (CRMs) were analysed along with samples to demonstrate the validity of the proposed analytical method. A certificate of analysis is provided for each CRM (Appendix 4 & 5). Detailed descriptions of the CRMs are provided in Table 3.2:

Table 3. 2: CRMs Description

Designation	Description	Source
CGL - 111	This REE ore originated from the Mushgia Khudag deposit, Umnogobi Province, Mongolia. In these rocks, most of the minerals are apatite and there is little secondary phosphate or hydrous ferric oxide to be found.	Central Geological Laboratory (CGL), Mongolia
CGL-124	This REE ore was extracted from the Lugiin Gol deposit in Dornogobi Province, Mongolia. With minor amounts of muscovite and potassium feldspar, it primarily consists of synchisite-bastnäsite, quartz, and dolomite	Central Geological Laboratory (CGL), Mongolia
AMIS0276	REE ore from Ampasindava Peninsula in the Antrasirana province of northen Madagascar. Comprised of tantalum, niobium, zirconium with enriched dykes hafnium, sills and argillaceous laterites.	African Mineral Standards (AMIS), South Africa

3.3. Materials and Reagents

Different acids with analytical grade HCL (37%), HNO_3 (65%), and HF (48%) were purchased from Chemical Enterprises such as (ACE) PTY LTD and Merck PTY LTD South Africa. All solutions were prepared using Millipore purified water (18 M Ω) for dilution of acids and samples as well as cleaning and rinsing of crucibles and glassware. Mars 6 CEM and Anton Paar 5000 multiwave microwave digestion instruments were used for acid digestion in this investigation.

3.4. Sample preparation for characterization

3.4.1. XRF & XRD sample preparation

From the collected sample, 8 g of each sample was weighed and mixed with 1.8 g of binder (the binder) into a clean dry squat beaker. The sample was mixed with a plastic rod to ensure that no sample was lost. The sample was then transferred into a milled bowel and milled for 3 minutes. The milled sample was transferred to an aluminum cup with a 32 mm diameter and then pressed into a pellet using a 10-ton pressing instrument for 2 minutes. Subsequently, the sample was analysed using a Rigaku WDX and XRF scan. The detection limits of the REEs on the XRF ranged between 0.1% and 100% ppm.

For XRD sample analysis, the sample was ground into a fine powder using a ball mill. The sample was placed into a clean and dry sample holder. The sample was then pressed down onto a flat surface to ensure that it was packed tightly and evenly. The sample was coated on the surface with a thin layer of adhesive to hold the powder during analysis. Then, the samples were labeled according to their date of preparation and information description before being loaded in the XRD instrument for analysis.

3.4.2. Scanning electron microscopy (SEM) – mineral liberation analysis

The sample preparation for scanning electron microscopy analysis was conducted by SJT MetMin services in Krugersdorp. The samples were prepared following the sample preparation procedures at SJT MetMin services. The samples were mounted in epoxy resin in 30 mm round polished blocks. The mounted resin blocks were polished and coated with carbon for examination by SEM. The coal ash samples had fine particles that tended to agglomerate during sample preparation. Therefore, paraffin was used to polish the particles during sample preparation to minimize

agglomeration. This is because paraffin would not dissolve or react with the sample particles.

The analysis of the prepared resin blocks was conducted at the University of Johannesburg in the Mineral Liberation Analyser laboratory. The analysis was performed using a scanning electron microscope FEI QUANTA 600 F instrument, which operates in a vacuum to ensure that there are no interactions with particles in the air. The instrument was operated in bright phase search mode in grid action to detect rare earth-bearing mineral phases. A back-scattered electron detector (BSE) was used at 25 kilovolts so that the elemental contrast could be used to locate the rare earth-containing carriers of interest. The BSE images were captured using MLA processing software. The working distance was kept at 13 mm, with each sample analyzed for 4 hours. The sample region evaluated by SEM was analyzed to determine the specific elements that are comprised using energy dispersive spectroscopy (EDS). The composition, grain size distribution, liberation, and mineral association were determined for the rare earth-bearing mineral phases and their surroundings using Esprit 1.9 software.

Figure 3. 2*:* scanning electron microscope FEI QUANTA 600 F instrument**.**

3.4.3. Open Hotplate Acid Leaching

Approximately 0.2 g of sample and CRMs were weighed into a 250 ml Teflon beaker, and the sample was water with water in the beaker. Then, 15 mL of HNO_3 and 5 mL of $HClO_4$ were added to 10 mL of HF, added to the beaker and heated for 5 hours at 230 °C. Then, the sample was cooled and transferred to a 50 ml volumetric flask.

3.4.4. Fusion leaching

Approximately 0.1997 – 0.2003 g of sample and CRMs were weighed into a 35 ml zirconium crucible, and 1.9997 – 2003 g of dry NaO_2 was added to 2 pellets of NaOH and mixed. Then, the sample was fused in a Bunsen burner (230 °C) until complete melt was achieved. Then, each crucible was

placed into a 250 ml beaker containing 10 ml of deionized water, and 10 mL of HNO_3 was added. Then, the sample was cooled and quantitatively transferred into a 50 mL volumetric flask.

3.4.5. Microwave-Assisted Digestion

Approximately 0.9997 – 0.2003 g of coal fly ash sample was weighed directly into Teflon-PFA digestion vessels, followed by the addition of 3 mL HCl, 9 mL HNO_3 and 3 mL HF. A closed vessel microwave heated for 40 minutes at a maximum temperature of 200 to 220°C was then used to digest the samples. The samples were left to stand at room temperature for 15 to 30 minutes before digestion.

Table 3. 3: Optimization condition set for Mar 6 microwave digestion

Steps	Power (W)	Ramp time (Minutes)	Temperature (º C)	Hold time (Minutes)
1	600	10	200	5
2	1000	5	220	30
3	1000	5	220	5

Table 3. 4: Optimization conditions for microwave digestion

Step	Power(W)	Ramp time (Minutes)	Temperature (º C)	Hold time (Minutes)
1	1200	20	200 - 220	40

Figure 3. 3: Mars 6 CEM and Anton Paar 5000 multiwave microwave digestion instruments.

After the solutions were allowed to cool to room temperature, they were transferred into 50 mL volumetric flasks and filled to the mark with deionized water prior to analysis of REEs on both the ICP–MS and ICP–OES.

3.4.6. Preparation of Standard Stock Solution

A standard stock solution of 1000 ppm with multirare earth elements was used to prepare a 1 ppm stock solution of REE standards. Calibration standards were prepared in 2% HNO_3. There was also an internal standard of 1 ppb g L^{-1} of Re and In included in each standard. Calibration standards were diluted according to the concentration range of I ppb to 100 ppb, as the calibration range consisted of five consecutive standards, as shown in Table 3.1.

Table 3. 5: Calibration standards and recovered ratio

Concentration	Calc Concentration	Ratio
0	0	-0.0011
5.0	5.095	0.6985
10.00	10.09	1.3844
20.00	20.114	2.7609
40.00	40.784	5.5992
50.00	48.935	6.7185
100.00	100.182	13.7556

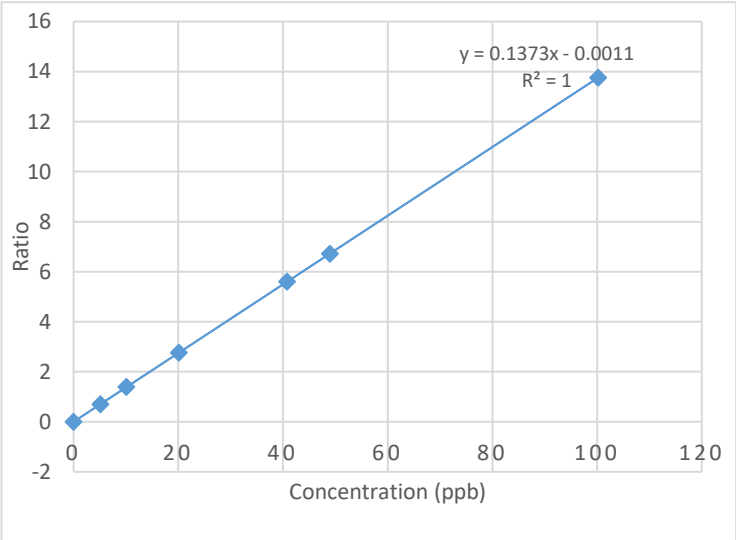

Figure 3. 4: Calibration Graph of the REE Standard

To prepare the sample for analysis, 1% HNO_3 solution was applied to the cones in the skimmer (Ni) before removal. Afterward, the instrument was calibrated with multielement REE standards. The calibration standards were prepared by dilution of 10 g L^{-1} standards of each REE in 2% HNO_3 (Inorganic Ventures). Re and In were also included as internal standards in each standard.

3.5. Sample preparation for elemental analysis in analytical techniques.

3.5.1. ICP–MS Instrument

ICP–MS analysis was performed on digested coal fly ash and REE CRMs from different digestion methods and fused samples. The samples were subjected to different dilution factors to check which dilution would optimize the sample matrix best. To analyse the samples, the most abundant isotopes were selected for each rare earth element, and In and Re were added as internal standards in each sample analysed to check whether the performance of the instruments was adequate or whether there were some deviations in instrument performance. To calibrate the instrument, various diluted fractions of standard solutions containing rare earth elements (REEs) were employed. These calibration standards are essential for ensuring the accuracy and precision of the analytical measurements during the instrument's operation. The concentrations of REEs corresponding to these fractions match the concentrations in Table 3.1; refer to Appendix 1 for calibration of the standard.

An analysis was performed for each analyte separately. The measurement sequence involves several steps, including the analysis of a blank sample, followed by the examination of a fraction of collected standards. This process is crucial for establishing a baseline (blank) and then assessing the performance of the instrument using known standards before analyzing the

actual samples, and a quality control check solution in accordance with the unknown amount of REE. A blank and CRM REE function was analysed in triplicate. After analysis, 2% HNO3 was used to clean the sample and skimmer cone of the instrument. This sequence was repeated before each subsequent analysis of a new analyte. It ensures that the instrument is properly calibrated and the measurement conditions are consistent for each element or sample being analyzed.

The instruments used for analysis were Thermo ScientificTM Q ICAP^{TM} (ICP-QMS) and Agilent ICP–MS 7800. Both instruments were optimized in two gas modes: kinetic energy discrimination (KED), which uses helium (He) gas during sample analysis, and standard (STD) mode, which uses argon (Ar) gas during analysis.

Figure 3. 5: Thermo ScientificTM Q ICAP^{TM} (ICP-QMS) instruments.

Table 3. 6: Thermo ScientificTM Q ICAP^{TM} (ICP-QMS) instrument operation conditions

Parameters	Conditions
Plasma power	1 400 - 1500 kW
Plasma gas	Argon & Helium
Plasma gas flow rate	17 L min-1
Auxiliary gas flow rate	1.4 L min-1

Nebulizer gas flow rate	0.75 L min-1
Data acquisition mode	Peak hopping
Sample uptake rate	0.8 mL min-1
Sampler cone	Copper (Cu)
Skimmer Cone	Nickel (Ni)
Acquisition time	100 s
Washout time	120 s
Number of replicates	3

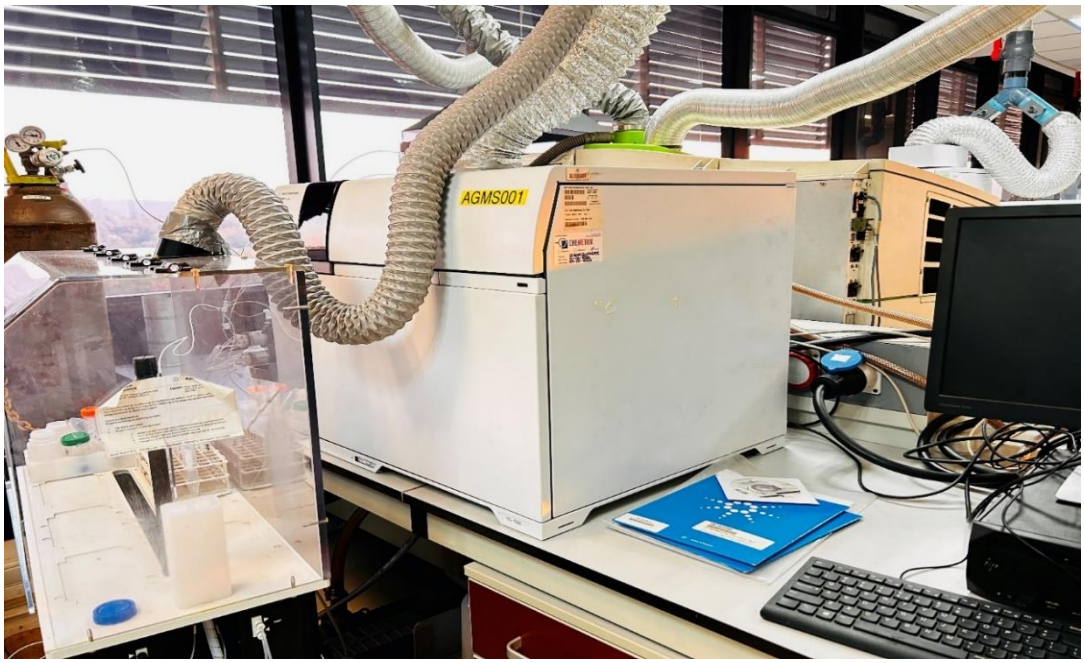

Figure 3. 6: Agilent ICP–MS 7800 instruments

Table 3. 7: Agilent MS HUNTER 7800 ICP–MS instrument operating conditions

Parameters	Conditions
Plasma power	1 400 kW
Plasma gas	Argon
Plasma gas flow rate	17 L min-1
Auxiliary gas flow rate	1.4 L min-1
Nebulizer gas flow rate	0.75 L min-1
Data acquisition mode	Peak hopping
Sample uptake rate	0.8 mL min-1
Sampler cone	Copper (Cu)
Skimmer Cone	Nickel (Ni)
Acquisition time	100 s
Washout time	120 s
Number of replicates	3

3.5.2. ICP–OES Instrument

The Agilent 5900 ICP–OES instrument was also used to perform REE analysis from the various methods.

An Agilent 5900 ICP–OES (Agilent Technologies Inc., California, United States of America) equipped with ICP-Expert software (version:

7.5.4.11997) and a charged coupled device detector (CCD) was used for the analysis of the REEs in solutions. The operating conditions (see Table 3.7) used were an RF power of 1.4 kW, a plasma current of 17 L min^{-1}, an auxiliary current of 1.4 L min^{-1} and a sample absorbance of 0.85 mL min^{-1}. Analysis was performed in radial mode for the REEs, with high-purity argon used as the plasma and carrier gas source. The wavelengths of the analytes are chosen according to their intrinsic strength and proximity to possible interferences. Calibration standards for REEs ranging from 0.5 to 1000 ppm, including calibration blanks, are prepared from mono-element stock solutions.

Figure 3. 7: Agilent 5900 ICP–OES instrument

Table 3. 8: Agilent 5900 ICP–OES instrument operating conditions

Parameters	Conditions
Plasma power	1 400 kW

Plasma gas	Argon
Plasma gas flow rate	17 L min-1
Auxiliary gas flow rate	1.4 L min-1
Nebulizer gas flow rate	0.85 L min-1
Sample uptake rate	1.5 mL min-1
Acquisition time	100 s
Washout time	120 s
Number of replicates	3

CHAPTER 4 RESULTS AND DISCUSSION

4.1 Characterisation of Fly ash samples

In this chapter, we aim to discuss the results of the objectives listed. These include optimizing conditions and characterization of the fly ash samples to determine the level of concentration in our feed samples, product minerals, and chemical properties present in collected fly ash samples. This chapter reviews and discusses the results from X-ray fluorescence (XRF), X-ray diffraction (XRD), and scanning electron microscopy (SEM) techniques.

4.1.1. X-ray Fluorescence Results

XRF analysis was conducted to identify the concentrations in the samples from the different coal power stations from the results obtained. The ash samples from the various power stations contained only LREEs in the range of 40 to 100 ppm (Table 4.1), while in Table 4.2 the mineral oxides ranged from 0.1 to 50%, with quartz being the major oxide. The presence of mineral oxide from all samples confirms that those ash samples are of high quality according to (11), as it determines the composition of ash chemicals (Shifeng et al. 2013). The XRF results for rare earth element analysis are presented in Tables 4.1 to 4.3.

Table 4.1 shows that all three fly ash samples contained rare earth elements despite their geological location. All three samples show a high content concentration of LREEs from XRF analysis, while HREEs were not detected from all different samples. The presence of mineral oxide from all samples in Table 4.2 confirms that those ash samples are of high quality according to Shifeng W, as it determines the composition of ash chemicals (Shifeng et al. 2013).

Other elements, such as Cr, Co, Ni, Cr, Zn, Ga, Rb, Y, Nb, W, Th, and Mo, showed high concentrations above 100 ppm in all samples. This was taken into consideration during sample preparation and analysis, as those elements can be considered high interferences in the determination of REEs.

Table 4. 1: Concentration of REEs in different power stations determined by XRF.

Sample ID	Kusile power station	Matla power station	Kandel power station
ELEMENTS	Concentration (ppm)		
La	104.7	65.9	97.6
Ce	191.2	138.1	185.8
Nb	33.8	37.1	39.2
Y	90.7	78.6	83
Ga	43.7	57.4	62.4

Table 4. 2: Major oxide composition determined in fly ash samples.

Sample ID	Kusile power station	Matla power station	Kandel power station
Oxides	**Mass (%)**		
Al2O3	31.74	24.81	31.24
SiO2	58.99	62.77	52.65
Fe2O3	4.444	4.573	3.615
CaO	7.6502	4.0312	5.8987
MgO	1.3948	0.7650	1.1457
Na_2O	0.3863	0.2220	0.1023

K_2O	1.0559	0.9815	0.7396
TiO_2	4.0516	3.8208	3.7855
P_2O_5	1.2761	0.6985	0.4467

4.1.2. X-ray Diffraction Results

XRD analysis was conducted to identify minerals that are present in the coal fly ash sample. The analysis showed that the sample consists predominantly of mullite with major amounts of quartz. The iron oxide magnetite is present in trace amounts (Table 4.3). The hump in the diffractogram (Figure 4.1) indicates the presence of amorphous content, as expected from the glass content in fly ash. The qualitative results relate only to the crystalline components identified. Overall, the fly ash sample is silicate-rich.

Table 4. 3: Qualitative XRD results of the mineral composition in the fly ash sample.

Mineral	Chemical Formula	Relative abundance
Quartz	SiO_2	major
Magnetite	Fe_3O_4	trace
Mullite	$Al_{4.52}Si_{1.48}O_{9.74}$	predominant

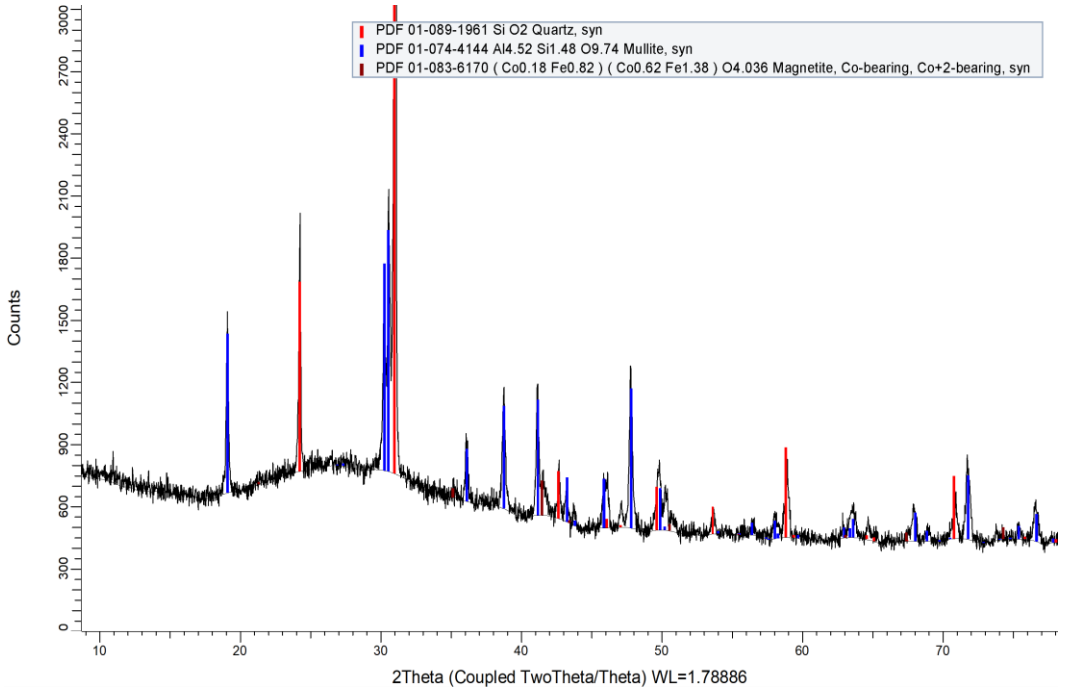

Figure 4. 1: Diffractogram of the fly ash sample showing the different mineral peaks present

The mineral composition in fly ash samples was mainly composed of quarts (SiO_2), mullite ($Al_{4.52}Si_{1.48}O_{9.74}$), magnetite ($Fe_3O_4$), and some quantity of pyrite (FeS_2), which were traced in the observation, as illustrated in Figure 4.1 above and the table 4.3. According to Xiuyi (2011), who conducted a study on coal to determine its mineral composition, the most abundant minerals found in coal and coal byproducts are quartz, kaolinite, calcite, and muscovite. Additionally, based on XRD (X-ray diffraction) analysis of coal samples and combustion products from the Tutuka power station in Mpumalanga, Akinyemi et al. (2012) identified quartz (SiO2), kaolinite (3Al2O3•2SiO2), and pyrite (FeS2) as the primary constituents of the coal (Mine et al. 2008; (Bank et al. 2016).

4.1.3. Scanning electron microscopy (SEM) analysis

Scanning electron microscopy (SEM) with energy dispersive spectroscopy (EDS) and automated backscattered electron (BSE) images were applied to a fly ash sample for the determination of minerals. This was done to determine if the fly ash contains REEs since the method is nondestructive in element sensitivity. The sample preparation for scanning electron microscopy analysis was conducted by SJT MetMin services in Krugersdorp as described in chapter 3.5.2.

The analytical work described in this context begins with the assessment of rare earth elements (REEs) minerals and their concentrations within a fly ash sample. This determination is carried out using a Backscattered Electron (BSE) image, as indicated in the image, employing a 25 kV acceleration voltage and a 10 nA beam current. The instrument selected a working distance of 12 mm. The gray feldspar color in the image below presents the REE-bearing minerals with high average atomic numbers and molecular masses. Following automated image analysis (as depicted in Figures A, C, and E), the electron beam is directed to the centroids of adjacent mineral grains, which are distinguished based on their Backscattered Electron (BSE) grey values. At this point, a single energy dispersive X-ray (EDX) spectrum is acquired, as illustrated in Figures B, D, and F. This process allows for the elemental analysis of the identified mineral grains.

When working with thin sections and polished blocks of ore, the image analyzer specializes in particle segmentation within a frame. It then generates a grid of individual Energy Dispersive X-ray (EDX) spectra, with each spectrum corresponding to a distinct contiguous domain characterized by its unique gray values. This measurement mode is often referred to as GXMAP, enabling the acquisition of EDX spectra from each identified

domain. The EDX spectra are normalized using the counting rates (counts per second, cts/s) of the associated EDX detectors. After normalization, the spectra are plotted against the keV (kilo-electronvolt) scale using the normalization method. This procedure ensures that the EDX data is appropriately adjusted and represented for analysis and interpretation. This EDX spectra has characteristic peaks at distinct keV positions as well as distinct relative cts/s, which indicates the elements present and their concentration semiquantitatively. In both measurement routines, geometrical and mineralogical parameters of particles and grains can be examined later, including size, shape, mineral locking, and mineral liberation.

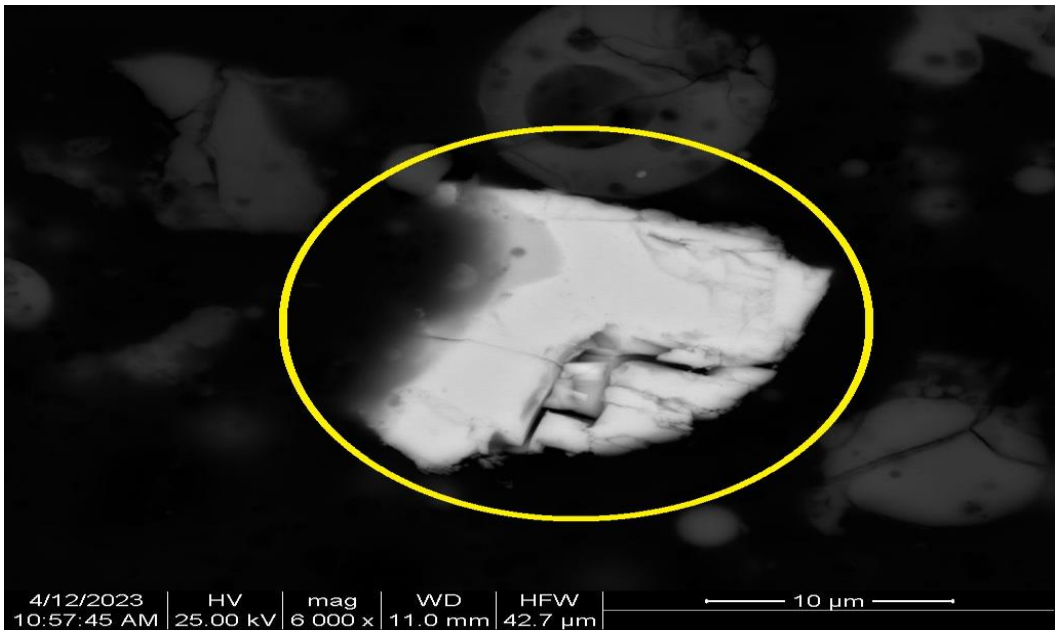

(A) BSE image of monazite

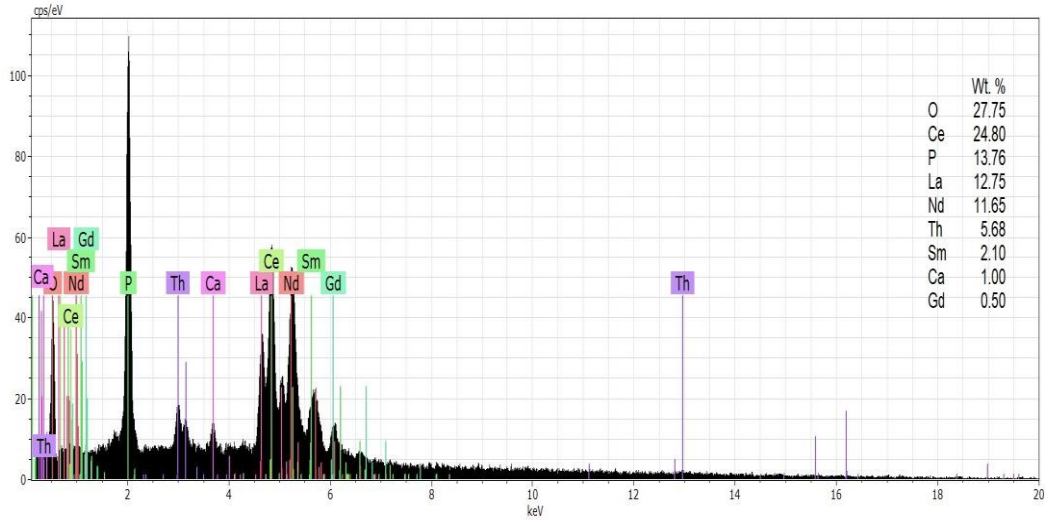

(B) EDX spectra of monazite

Figure 4. 2: (A; BSE image of monazite mineral, B; EDX spectra of monazite)

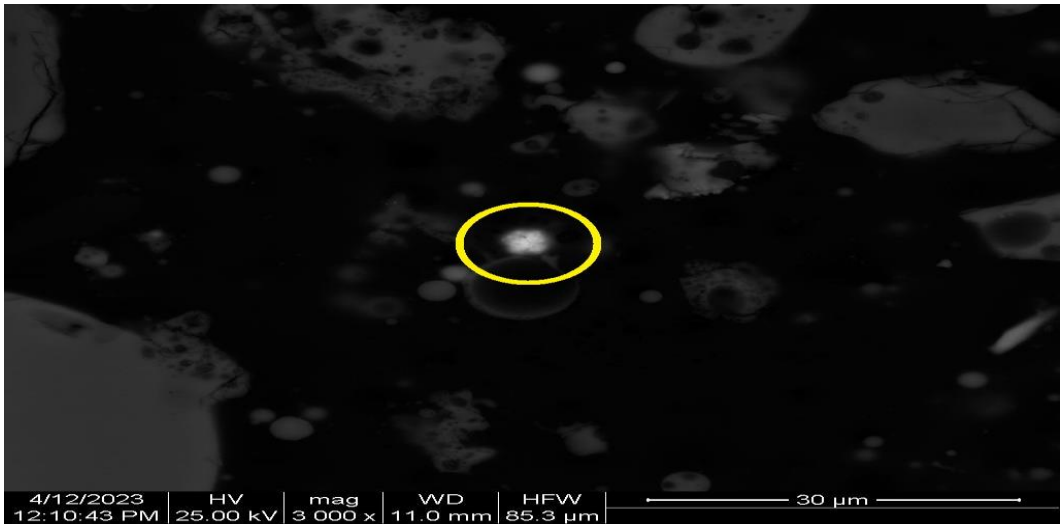

(C) BSE image of perrierite mineral

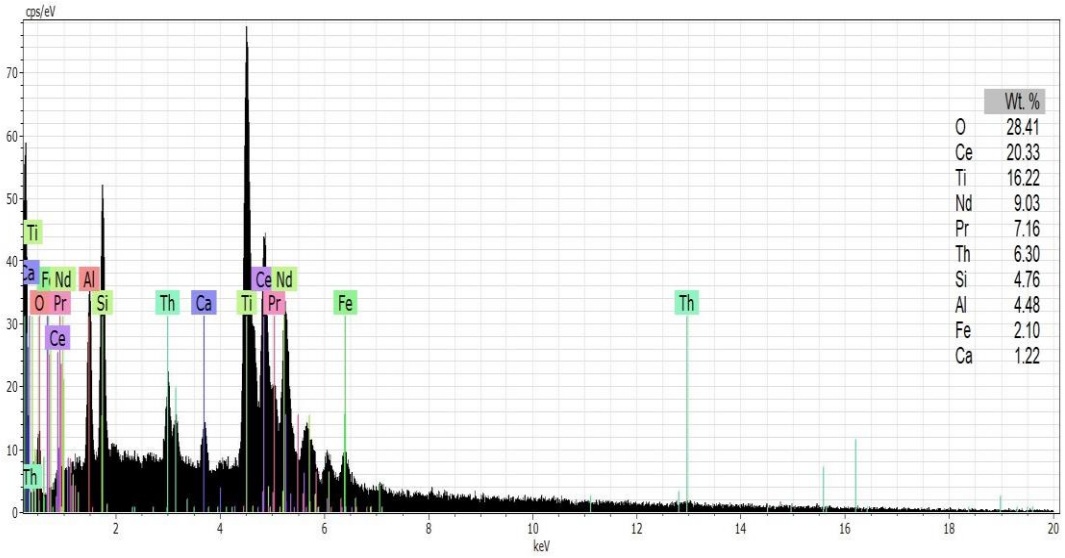

(D) EDX spectra of perrierite

Figure 4. 3: (C; BSE image of perrierite mineral, D; EDX spectra of perrierite)

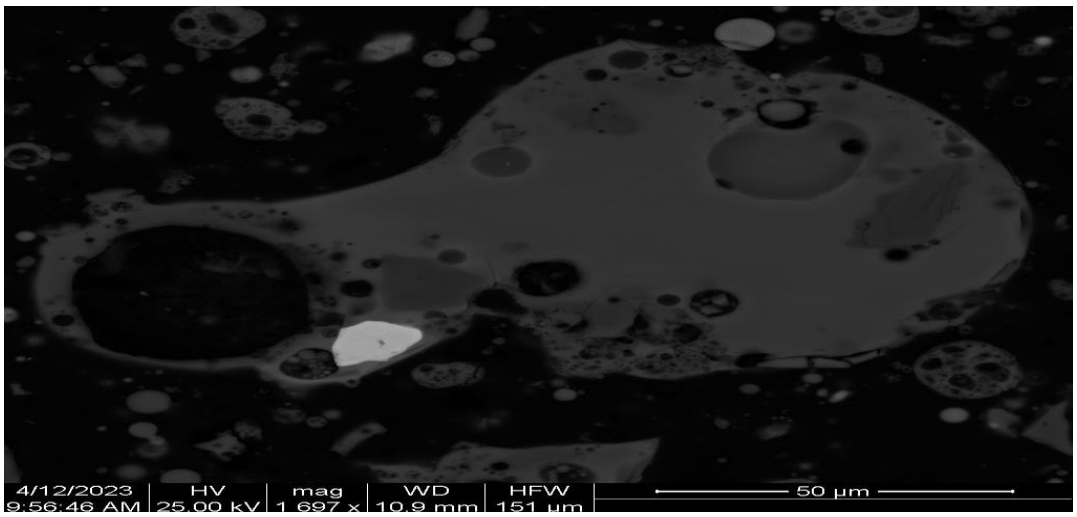

(E) BSE image of xenotime

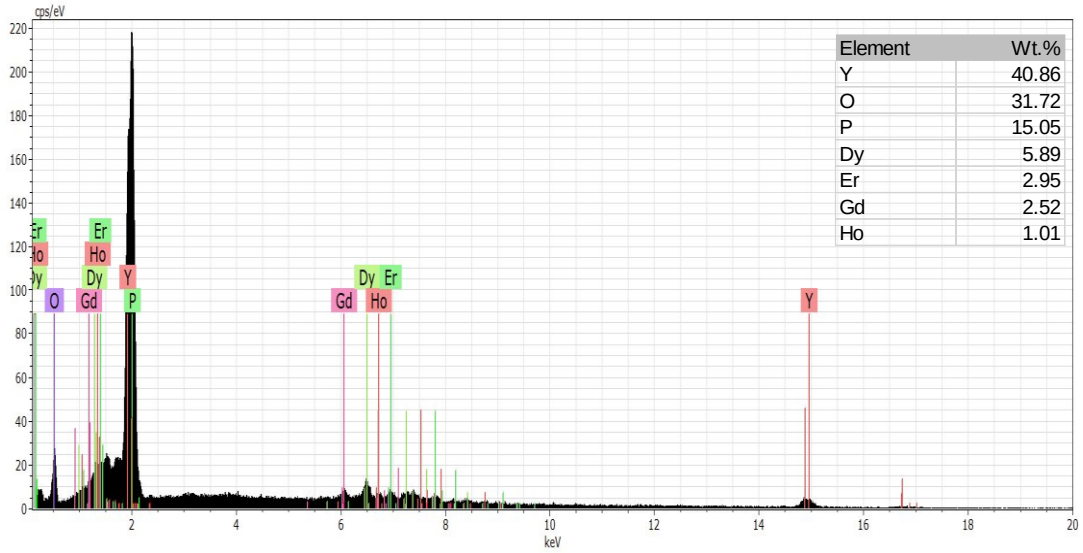

(F) EDX spectra of xenotime

Figure 4. 4: (E; BSE image of xenotime, F; EDX spectra of xenotime)

Figure 4.2 The EDX spectra show the concentration of elements associated with the monazite mineral found in Wt % (O:27.75, Ce:24.80, P:13.76, La:12.75, Nd:11.65, Th:5.68, Sm:2.10, Ca:1.00, Gd:0.50). Figure 4.3 (C) shows the BSE image of perrierite mineral, followed by (D), which is the corresponding spectra with the labeled elements in Wt% (O:28.41, Ce:20.33, Ti:16.22, Nd:9.03, Pr:7.16, Th:6.30, Si:4.76, Al:4.48, Fe,2.10, Ca,1.22).

Figure 4.4(E) shows the BSE image of the xenotime mineral, and (F) shows the spectra of xenotime with corresponding elements in Wt % (Y:40.86, O:31.72, P:15.05, Dy 5.89, Er:2.95, Gd:2.52, Ho,1.01).

4.1.4. Chapter conclusion

As outlined above, the composition of REE-bearing minerals can be rather complex because they contain complex chemical elements. This is also evidence that mineral and chemical diversity can also be seen in the most important economic REEs because of their mineral bearing. The overall analysis shows that the fly ash is a siliceous-rich sample with the most abundant minerals, quartz (SiO_2), magnetite (Fe_3O_4), and mullite ($Al_{4.52}Si_{1.48}O_{9.74}$). A study performed by Franus on XRD found that fly ash ashes from bituminous coal showed the presence of mullite and less quartz and iron oxides (hematite and magnetite) (Wojciech. et al. 2015)

The rare earth element (REE) phosphate known as monazite, which contains light rare earth elements (LREE), yttrium (Y), thorium (Th), silicon (Si), and calcium (Ca), exhibits a significant variation in the concentration of LREE elements. Specifically, it has varying concentrations of cerium (Ce), lanthanum (La), neodymium (Nd), and samarium (Sm), which are part of the LREE group. The xenotime (Y, HREE) PO_4 mineral liberation shows a high concentration of HREE elements (Y, Dy, Er, Gd, Ho). Perrierite minerals showed possible identification of LREEs (Ce, Nd, and Pr) with possible other mineral species containing elements such as O, Ti, Th, Si Al, Fe, and Ca.

Bulk chemical analysis of fly ash samples and processing by X-ray fluorescence (XRF) and X-ray diffraction (XRD) successfully identified minerals and elemental concentrations in fly ash samples. However, In a mineral composition-based approach, you are left with a long and confusing list of mineral names. Since mineral compositions can be complex and mineral names can be unwieldy, it is difficult to identify individual REE minerals accurately. Sandmann *et.al,* (2019) did a study on how SEM-based automated mineralogy and its application on geo-materials including

coal for the determination of REEs, on their finding they observed that REE minerals such as monazite, and xenotime are highly liberated with REE elements, while other minerals such as perrierite and kaolinite showed a presence of other chemical species (Schulz, Merker, and Gutzmer 2019).

4.2 Elemental analysis of Fly Ash samples

This section presents the results interpretation of collected data as described in Chapter 3 for elementary analysis by ICP–MS and ICP–OES. The presented results are in the form of graphs, table format, and then discussed.

4.2.1 ICP–MS and ICP–OES

ICP MS and ICP–OES techniques were used to determine the concentration of REEs in the fly ash samples. Before the analysis of each CRM and sample, calibration of the instruments was performed using a multirare earth element standard. This was done to ensure that the instrument was adequate to respond to the analytes of interest. The regression plot obtained for all REEs ranged from R^2 = 0.9997 – 1.0, as illustrated in Figure 4.5. below. For all individual calibrations for REEs, refer to Appendix 1.

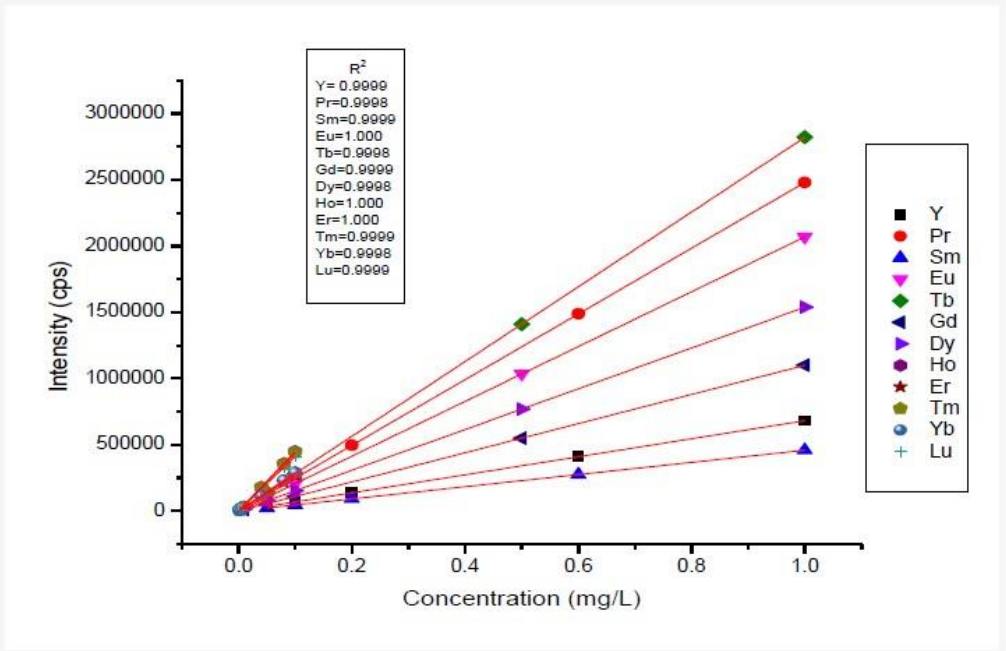

Figure 4. 5: **Regression plot for REEs at various concentration ranges**

4.2.2 Certified Reference Material (CRMs) Results for Validation

Three CRMs, CGL 111, CGL 124, and AMIS0276, of REEs were selected and used as part of validating techniques used for the determination of REE concentrations as described in chapter 3.2. Vales of each CRM concertation obtained were compared against the certified values and calculated percentage recovery (%).

The recovered results from the microwave acid digestion method (HNO_3, HCl, and HF) used for digestion in selected CRMs (CGL 111, CGL 124, and AMIS0276) were well digested as described in Chapter 3.2. The digestion method was iterated over multiple trials (n=10) to optimize the microwave conditions and enhance the recovery of rare earth elements (REEs) in the selected certified reference materials (CRMs). The aim was to align the

results with the certified values, indicating a high level of accuracy and precision in the analytical process. The obtained results, in conjunction with the certified values, were employed to calculate the percentage recovery (%) of rare earth elements (REEs) for all three chosen certified reference materials (CRMs), as outlined in Tables 4.4 to 4.6. The recovery was determined through the following calculation method:

$$\%\text{Recovery} = \frac{Obtanied\ value}{Certified\ value} \times 100\% \quad (2)$$

Table 4. 4: Statistical evaluation of results obtained by ICP MS for CGL 111 REEs CRM in microwave acid digestion.

Elements	Measured Con ppm	Certified Con ppm	95% Confidence Limits ppm		Mass selected Isotope	% Recovery
			Low	High		
Y	900.4899	959	884	1034	89	93.90
La	18927.7	19300	17448	21307	139	98.07
Ce	28600.71	29000	26655	31552	140	98.62
Pr	2676.076	2800	2454	3040	141	95.57
Nd	8677.113	8900	8010	9790	146	97.50
Sm	835.773	900	788	1012	147	92.86
Eu	199.763	212	185	239	153	94.23
Tb	57.359	55	39.7	70.3	159	104.29
Gd	558.745	553	501	605	156	101.04
Dy	186.669	206	181	231	163	90.62
Ho	39.507	37	29.9	40.7	165	106.78
Er	75.08	80	72	88	166	93.85
Yb	55.545	55	49.7	60.3	172	100.99

NB: Con= concertation (ppm)

Table 4. 5 : Statistical evaluation of results obtained by ICP MS for CGL 124 REEs CRM in microwave acid digestion.

Elements	Measured Con ppm	Certified Con ppm	95% Confidence Limits ppm		Mass selected Isotope	% Recovery
			Low	High		
Y	201.0581	167	109	225	89	120.39
La	21943.13	21100	19196	22999	139	104.00
Ce	26745.72	27600	26222	29220	140	96.90
Pr	2412.472	2300	2180	2420	141	104.89
Nd	6774.122	6500	6125	6841	146	104.22
Sm	500.572	539	485	593	147	92.87
Eu	85.552	87	78.3	95.7	151	98.34
Tb	41.355	45	38.2	51.8	159	91.90
Gd	292.825	295	232	358	157	99.26
Dy	59.256	58	52.2	63.8	163	102.17
Ho	8.486	8	7.2	8.8	165	106.08
Er	20.809	24	19.9	21.8	166	86.70
Yb	16.32	18	14.2	21.5	172	90.67

NB: Con= concertation (ppm)

Table 4. 6: Statistical evaluation of results obtained by ICP MS for AMIS0276 REEs CRM in microwave acid digestion.

Elements	Recovered Con ppm	Certified Value ± 95% Confidence Limits ppm	Mass selected m/z	% Recovery
Y	44.489	46.6 ± 60	89	95.49
La	79.063	76.6 ± 8.1	139	103.22
Ce	237.594	208 ± 42	140	114.23
Pr	16.067	15.3 ± 1.1	141	105.01
Nd	52.972	53.8 ± 4.3	143	98.46
Sm	9.382	9.7 ± 0.9	147	96.72
Eu	1.026	1.37 ± 0.16	153	102.64
Tb	1.696	1.2 ± 0.1	159	141.33
Gd	8.370	8.4 ± 1.2	157	99.65
Dy	8.839	8.4 ± 0.7	163	105.22
Ho	2.108	1.8 ± 0.1	165	111.11
Er	5.770	5.4 ± 0.4	166	105.55
Yb	3.018	3.4 ± 0.3	173	88.52
Lu	0.363	0.5 ± 0.1	176	72.6

NB: Con= concertation (ppm)

The results of the REE concentration from all reference selected CRMs obtained from ICP–MS through microwave acid digestion methods show good recovery, as shown in Table 4.4 to Table 4.6, and Figure 4.6. The optimization shows a good response for both the microwave and ICP-MS instruments.

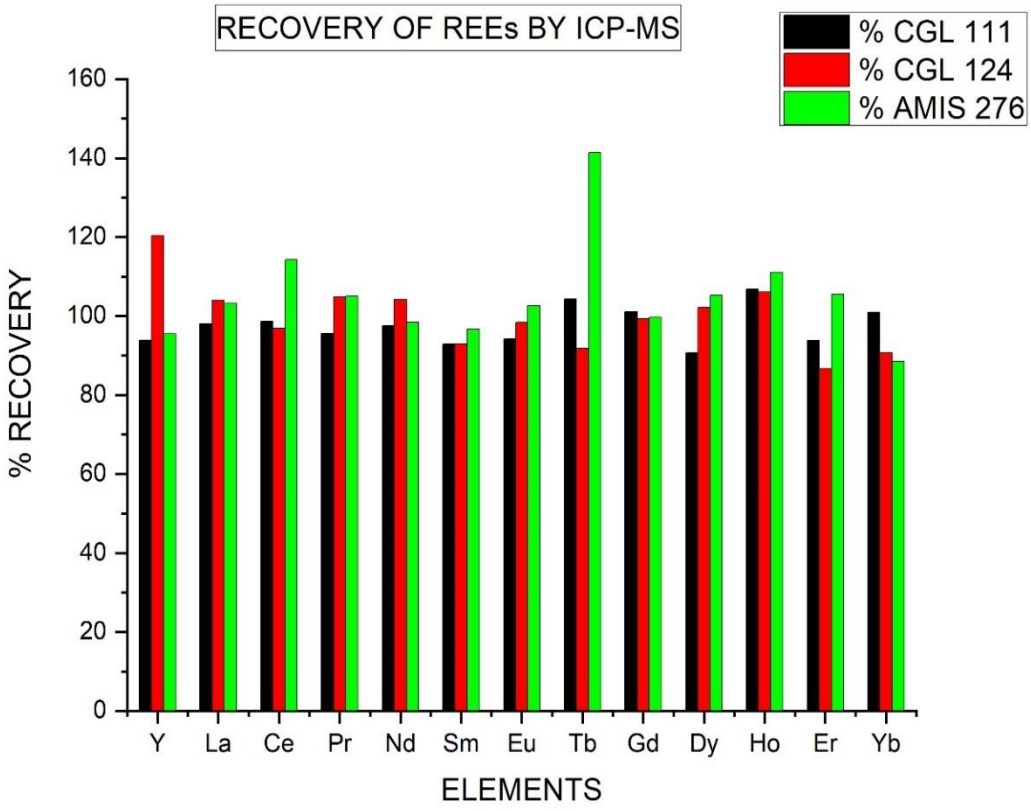

Figure 4. 6:% Comparison of the different CRM recoveries by microwave and ICP–MS.

Table 4.7 represents the percentage (%) results from the sodium peroxide fusion method. The method was applied in selected CRMs to check and compare the percentage recovery between the two methods. Both methods were found to produce good results. with a percentage recovery between 80-120% in ICP–MS analysis, as illustrated in Figure 4.6. However, the sodium peroxide method was not applicable in ICP–OES analysis due to a low recovery, which was observed during the initial stage of analysis. This was caused by the formation of a high silica precipitate in the preparation of the sample solution. which then caused a blockage in the nebulizer during the analysis. Additionally, there is a high amount of interference due to overlapping wavelengths (ʎ) between elements.

Table 4. 7 :Calculated percentage recovery (%) for results obtained by ICP MS for CGL 111 and 124 REEs CRM from sodium peroxide Fusion.

Elements	% Recovery CGL 111	% Recovery CGL 124	% Recovery AMIS0276
Y	102.09	77.70	N/A
La	92.84	96.92	N/A
Ce	99.24	105.06	N/A
Pr	89.65	102.01	N/A
Nd	92.92	103.75	N/A
Sm	89.79	94.38	N/A
Eu	90.32	100.07	N/A
Tb	71.35	87.21	N/A
Gd	102.13	96.18	N/A
Dy	89.63	93.85	N/A
Ho	97.88	100.66	N/A
Er	100.48	101.12	N/A
Yb	99.35	107.41	N/A

NB: N/A= AMIS0276 results were not available for sodium peroxide fusion

Table 4. 8: Calculated percentage recovery (%) for results obtained by ICP–OES for CGL 111 and 124 REEs CRM from microwave acid digestion

Elements	% Recovery	% Recovery	% Recovery
	CGL 111	CGL 124	AMIS0276
Y	103.4244	106.9701	105.1972
La	99.56746	97.76408	98.66577
Ce	103.8623	99.90098	101.8816
Pr	92.70714	96.3887	94.54792
Nd	118.719	110.6966	114.7078
Sm	90.73333	93.62152	92.17743
Eu	95.21226	102.4138	98.81303
Tb	140.1091	132.2889	136.199
Gd	101.3363	88.79661	95.06648
Dy	92.29126	108.6552	100.4732
Ho	81.21622	108.75	94.98311
Er	69.15	61.41667	65.28333
Yb	101.0545	118	109.5273

ICP–OES also shows low sensitivity in low-REE CRMs, as observed in AMIS0276. The instrument was underrecovering the CRM values due to a lack of sensitivity in the low-concentration REE sample. The instruments show a good trend and reproducibility in highly concentrated REE CRMs such as CGL 111 and CGL 124, as illustrated in Figure 4.7 below.

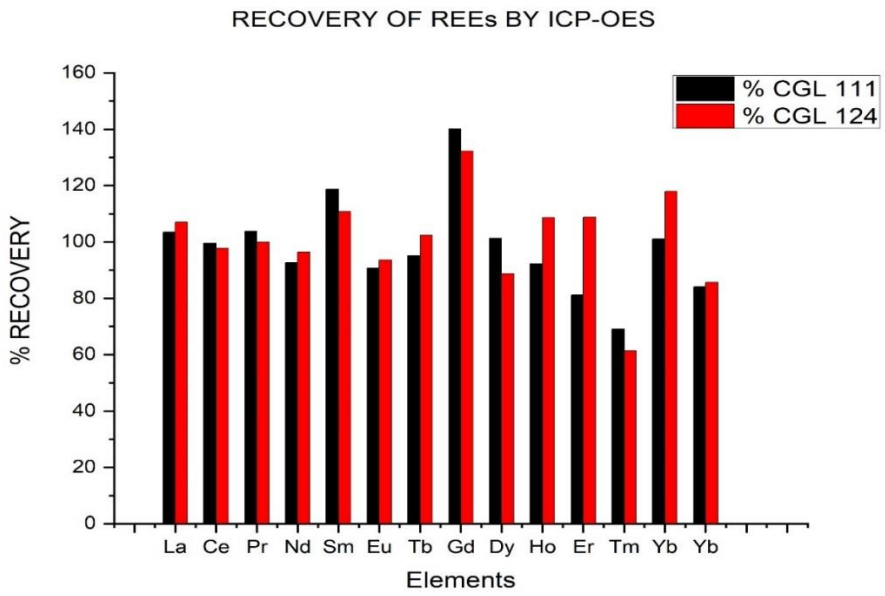

Figure 4. 7: % Recovery of REEs from CRMs by ICP–OES

The recovery of rear earth elements from REE CRMs was successful. To obtain the best possible applicable digestion methods and analytical techniques for the analysis of REEs. Three internationally certified reference materials (CRMs) were used (CGL 111. 124 & AMIS0276) to develop closed vessel methods that can be employed to analyse REE samples from fly ash samples. After setting suitable parameters in the microwave digestion method. REEs were quantitively recovered using the acid digestion method in a closed vessel condition and analysed by ICP–MS and OES instruments. ICP–MS showed good recoveries (80 – 120%) for most major trace elements compared to ICP–OES-OES analysis, in which the recovery was approximately 50 -120%, as illustrated in Figure 5.4 below.

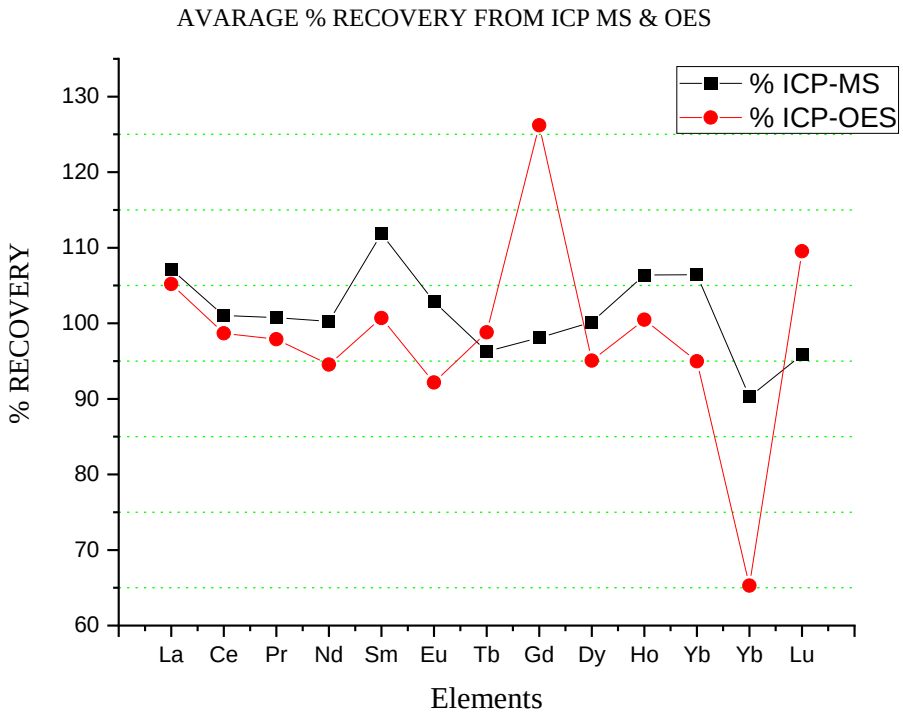

Figure 4. 8: Comparing average % between ICP MS & OES analysis

The recovery of rear earth elements from REE CRMs was successful. To obtain the best possible applicable digestion methods and analytical techniques for the analysis of REEs. Three internationally certified reference materials (CRMs) were used (CGL 111. 124 & AMIS0276) to develop closed vessel methods that can be employed to analyse REE samples from fly ash samples. After setting suitable parameters in the microwave digestion method. REEs were quantitively recovered using the acid digestion method in a closed vessel condition and analysed by ICP–MS and OES instruments. ICP–MS showed good recoveries (80 – 120%) for most major trace elements compared to ICP–OES-OES analysis, in which the recovery was approximately 50 -120%, as illustrated in Figure 4.8 above.

The observation seen in all data obtained shows that ICP–MS results can be considered more reliable through this technique in the determination of REEs in closed vessel acid digestion. This is because the instrument shows a good recovery in all REE elements, whether LREEs or HREEs. Whereas the results from ICP–OES showed lower recovery compared to ICP MS, the ICP–OES instruments showed a good recovery in LREEs compared to HREEs. Overall observation from the obtained results in both techniques applied in the determination of REEs by assisted microwave acid digestion methods showed good recovery. most of the elements were within the accepted value of 95% confidence intervals as provided by the certificate of applied CRMs. ICP-MS is a common technique that was used to determine the REE concentration in fly ash samples since the results of validation through CRMs showed good recovery.

4.2.3 REE results from fly ash samples

All three acquired fly ash samples were subjected to microwave acid digestion and sodium peroxide fusion methods to recover the REE concentration. The samples were analysed using the ICP–MS technique, as it was the technique that showed good recovery through the validation process compared to ICP–OES.

Table 4. 9: ICP–MS results for fly ash samples from microwave acid-assisted digestion and sodium peroxide fusion.

Elements	Measured Concentration (ppm)					
	KUSILE		MALTA		KENDAL	
	Acids	Fusion	Acids	Fusion	Acids	Fusion
Y	63.75	57.44	53.25	56.66	53.50	62.70
La	154.91	154.50	112.02	117.00	120.05	118.24
Ce	197.84	203.29	193.38	192.97	197.96	192.69
Pr	21.48	22.61	23.92	20.89	21.89	20.27
Nd	86.57	92.16	99.17	88.60	85.80	83.23
Sm	15.12	16.64	18.39	15.67	15.95	16.07
Eu	2.515	2.54	2.68	2.605	2.31	2.739
Tb	4.215	5.68	5.18	5.37	5.36	5.00
Gd	15.74	15.01	12.18	15.57	14.13	16.64
Dy	14.57	14.60	15.37	13.97	14.38	15.63
Ho	1.70	1.89	2.02	1.843	1.98	2.01
Er	8.02	7.37	7.87	7.35	7.50	7.98
Tm	0.73	0.74	0.71	0.707	0.70	0.70
Yb	3.741	3.85	3.29	3.91	4.10	4.03
TREE	598.10	435.88	549.00	446.49	556.00	525.16

NB: TREE= Total RareErth Elements

From the obtained results, there is a slight difference between the concentrations of REEs in all three different samples from the Kusile, Malta, and Kendal power stations. The samples showed similar concentration levels for all the elements. All three samples showed a high concentration level of LREEs (Y, La, Ce, and Nd) ranging between ~50 ppm to ~200 ppm, whereas the HREE (Sm, Eu, Tb, Gd, Dy, Ho, Er, and Yb) concentration was lower throughout all samples, ranging between ~0.5 ppm to ~20 ppm, as illustrated in Table 4.9 and Figure 4.9. The concentration of REEs from both

acid digestion and fusion methods showed similar concentrations in all samples, as observed in Table 4.9.

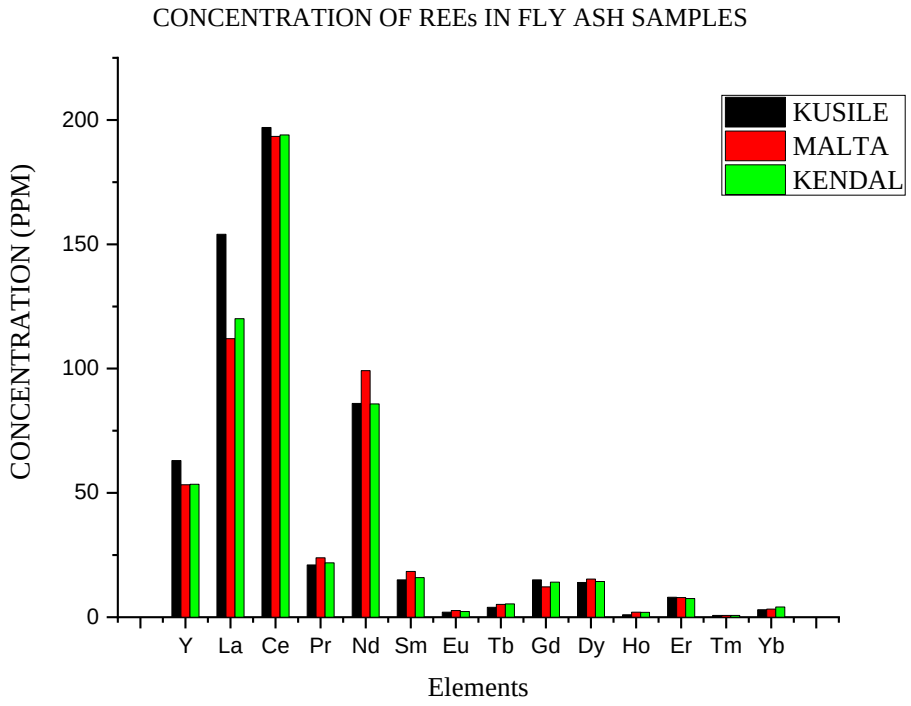

Figure 4. 9: Determine concentrations of REE in various samples by ICP–MS

From the obtained results. There is a slight difference between the concentrations of REEs in all three different samples from Kusile. Malta. and Kendal power stations. The samples showed the same concentration level of all elements. All three samples showed a high concentration of LREEs (Y. La. Ce. Nd) ranging between 50 ppm to 200 ppm. whereas HREEs (Sm. Eu. Tb. Gd. Dy. Ho. Er. Yb) concentration was lower throughout all samples, ranging between 0.5 ppm to 20 ppm, as illustrated in Table 4.9 and Figure 4.9. The concentration of REEs from both acid digestion and fusion methods showed almost the same concentration in all samples, as observed in Table 4.9. Other studies reported by (Ketris and Yudovich 2009) and (Wojciech.

et al. 2015) show similar concentration determination from different coal fly ash.

The total REE (TREE) concentration in all ash samples, as shown in Figure 4.10 for both acids and fusion methods, ranges between 400 ppm to 600 ppm. Kusile power station samples appear to be more concentrated (~600 ppm), and Malta and Kendal power station samples show almost the same concentration (~ 450 ppm). Overall, the ash samples exhibited a total rare earth element (REE) concentration that was approximately equal to or greater than the average global baseline concentration of 445 ppm. This suggests that the REE content in these samples was consistent with or higher than the typical global average. According to a study done by (Ostrovnaya et al.2013), the concentrations of different fly ash typically range between 0.5 ppm to 200 ppm.

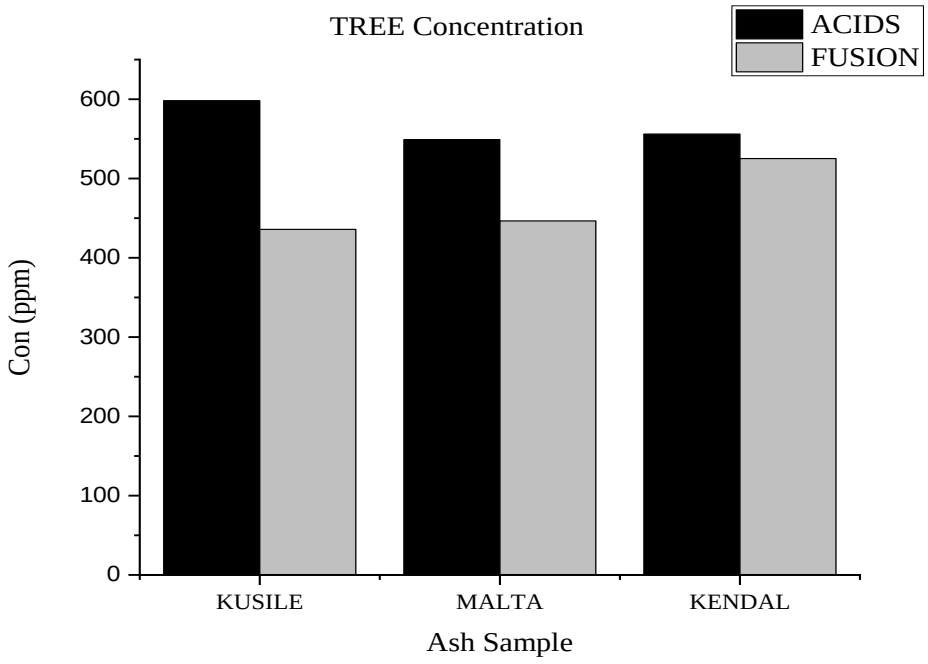

Figure 4. 10: Total REE concentration in fly ash samples from acid digestion and sodium peroxide fusion.

4.2.4 Chapter Summary

The results presented in this chapter demonstrate that the ICP-MS instrument provides superior results for rare earth elements (REEs) compared to both the microwave multi-acid digestion and the sodium peroxide fusion methods. This suggests that ICP-MS is the more effective analytical technique for REE analysis in this context. With the use of certified reference materials, we made a comparison of the results obtained by using these two digestion techniques CGL 111, CGL 124, and AMISO276 to validate whether the methods are reliable.

The recovery percentage (%) from ICP–MS showed a good percentage yield (80 – 120%) compared to the ICP–OES instrument (50 – 120%). The ICP–MS data indicate that all fly ash samples have a high concentration of LREEs and a lower concentration of HREEs. Excellent recovery was obtained by ICP–MS in a developed microwave acid digestion method.

CHAPTER 5: CONCLUSION AND RECOMMENDATION

The chapter covers major findings, challenges, and successes observed in the study. Recommendations are also stated for future studies and improvements.

5.1. Conclusion

To achieve the goals and aim of this study. Three different fly ash samples were successfully collected from three different power stations. Samples were characterized by XRF and XRD followed by ICP–MS and ICP–OES quantification.

- The aim and objectives of the study were successfully met and demonstrated.
- Optimization of the sample through microwave multiacids was successful, as the results of selected REEs in CRM (CGL 111, CGL 124, and AMISO276) obtained from ICP–MS and ICP–OES-OES showed good recovery compared with certified values.
- The utilization of certified reference materials to assess the analytical performance using selected techniques has yielded favorable results, indicating a reliable and accurate response from the analytical methods employed.
- Results imply that the microwave acid digestion method is a more efficient way of preparing samples and it generates acceptable results for various analytical procedures. Because, when compared to the fusion approach, the microwave acid digestion method consistently produces outstanding results in ICP-MS and ICP-OES.
- The ICP–MS technique was able to recover REEs from both applied methods more accurately than ICP–OES, which only showed a better recovery in acid digestion methods. Recovery for ICP–MS was approximately 80 – 120%, whereas ICP–OES was around 50- 120%.
- Microwave acid digestion recovers REE more efficiently and quicker than sodium peroxide fusion methods, as observed in the investigation.
- All three fly ash samples were found to be more concentrated with LREEs than HREEs. The total REE (TREE) concentration in all

samples was found to range from 400 ppm to 600 ppm, which agrees with the literature.

5.2. Recommendation

From the results obtained in this study. It is recommended that further studies and research be done in the future to improve some of the findings, such as the following:

- Furthermore,the is a need to find ways of enhancing the recovery of rare earth elements for ICP –OES analysis. This indicates ongoing efforts to optimize the analytical process and improve the accuracy of REE measurements with the ICP-OES technique.
- Obtain suitable certified reference materials (CRMs) with a similar matrix as the fly ash samples to ensure the quality and accuracy of the analytical process. This involves using reference materials that closely resemble the composition and properties of the fly ash for validation and quality control.
- Explore additional extraction methods to improve the separation of rare earth elements (REEs) from other components, ultimately leading to enhanced recovery and precision in REE analysis.

References

Adams, ., and Ward, J. 2015. “Beneficial Use of Coal Combustion Products: An American Recycling Success Story.” American Coal Ash Association, 38800 Country Club Drive Farmington Hills, MI 48331.”

Al, Çelik AYaman HTuran S. et. 2018. “Analytical Determination of REEs in Coal Fly Ash and Its Application in Two REE Recovery Processes: Aqueous Leaching and Plasma Arc Gasification.” *Journal of Materials Processing Technology (* 1(1) 1-8:1(1) 1-8.

Anon. 2012. . “. Retrieved From:” *Facilitating Learning Through Humour At a Nursing Education Institution in Gauteng*.

Baker, Lucy, Jesse Burton, Catrina Godinho, and Hilton Trollip. 2015. “The Political Economy of Decarbonisation : Exploring the Dynamics of South Africa’s Electricity Sector.” (November). doi: 10.13140/RG.2.1.4064.9040.

Balaram, V. 1996. “Recent Trends in the Instrumental Analysis of Rare Earth Elements in Geological and Industrial Materials.” *TrAC - Trends in Analytical Chemistry* 15(9):475–86. doi: 10.1016/S0165-9936(96)00058-1.

Bank, Tracy, Elliot Roth, Phillip Tinker, Evan Granite, Tracy Bank, Phillip Tinker, and Evan Granite. 2016. “Analysis of Rare Earth Elements in Geologic Samples Using Inductively Coupled Plasma Mass Spectrometry US DOE Topical Report - DOE / NETL-2016 / 1794 Analysis of Rare Earth Elements in Geologic Samples Using Inductively Coupled Plasma Mass Spectrometry.”

Bartlett, Nicholas J. 2011. “Critical Materials Strategy for Clean Energy

Technologies.” *Critical Materials Strategy for Clean Energy Technologies* 1–170.

Bunaciu, Andrei A., Elena Udriştioiu, Hassan Y. Aboul-enein, Andrei A. Bunaciu, Elena Udriştioiu, Hassan Y. Aboul-enein, Andrei A. Bunaciu, and Elena Gabriela Udri S. 2015. “Critical Reviews in Analytical Chemistry X-Ray Diffraction : Instrumentation and Applications X-Ray Diffraction : Instrumentation and Applications.” 8347. doi: 10.1080/10408347.2014.949616.

Derkach, Tetiana M., and Olga P. Baula. 2017. “Вісник Дніпропетровського Університету . Серія Хімія Bulletin of Dnipropetrovsk University . Series Chemistry PHARMACOPOEIA METHODS FOR ELEMENTAL ANALYSIS OF MEDICINES : ПОРІВНЯЛЬНЕ ДОСЛІДЖЕННЯ Анотація ФАРМАКОПЕЙНЫЕ МЕТОДЫ АНАЛИЗА ЭЛЕМЕНТОВ В ЛЕКАРСТВЕНН.” 25(2):73–83. doi: 0.15421/081711.

Drobne, Damjana, Sara Novak, Iva Talaber, Iseult Lynch, and Anita Jemec Kokalj. 2018. “The Biological Fate of Silver Nanoparticles from a Methodological Perspective.” 1–26.

Du, Xiaoyue, and T. E. Graedel. 2011. “Uncovering the Global Life Cycles of the Rare Earth Elements.” *Scientific Reports* 1:1–4. doi: 10.1038/srep00145.

Editor, David A. Atwood. 2013. “The Rare Earth Elements : Fundamentals and Applications.”

Eskom. 2021. “Integrated Report - 31 March 2021.” (March):75.

Frandsen, Flemming. 1997. “Empirical Prediction of Ash Deposition Propensities in Coal-Fired Utilities.”

Franus, Wojciech, Ma M. Wiatros-motyka, and Magdalena Wdowin. 2015. “Coal Fly Ash as a Resource for Rare Earth Elements.” 9464–74. doi: 10.1007/s11356-015-4111-9.

Gholz, E. 2014. “Rare Earth Elements and National Security.” *Energy Report* (October):1–20.

Gupta, G. K., and N. Krishnamurthy. 1992. *Extractive Metallurgy of Rare Earths*. Vol. 37.

Hancox, P. J. 2016. “The Coalfields of South-Central Africa : A Current Perspective.” (2005):407–28. doi: 10.18814/epiiugs/2016/v39i2/95785.

Henderson, P. 1984. “RARE E A R T H ELEMENT.”

Hou, Xiandeng, Renata S. Amais, Bradley T. Jones, and George L. Donati. 2017. “Inductively Coupled Plasma Optical Emission Spectrometry.” *Encyclopedia of Plasma Technology* 655–78. doi: 10.1081/e-eplt-120052737.

Huang, Chunhui, and Zuqiang Bian. 2010. “CO.” 1–40.

Hurst, Cindy. 2010. “China’s Rare Earth Elements Industry: What Can the West Learn?” *Institute for the Analysis of Global Security (IAGS)* (March):43.

January, Congress. 2017. “Report on Rare Earth Elements from Coal and Coal Byproducts.” (January).

Jeremy DreierA., Henry, Josette LaCaria, and Jeannine Howatt. 2009. “Coal Ash: Characteristics, Management and Environmental Issues.” (September).

JoVE, Cambridge, MA. 2023. “X-Ray Diffraction for Determining Atomic and

Molecular Structure _ Materials Engineering _ JoVe.”

Justin, Joseph, and Mbenza Muaka. 2013. “Ground Stresses in the Coalfields and Their Impact On.”

Ketris, M. P., and Ya E. Yudovich. 2009. “International Journal of Coal Geology Estimations of Clarkes for Carbonaceous Biolithes : World Averages for Trace Element Contents in Black Shales and Coals.” *International Journal of Coal Geology* 78(2):135–48. doi: 10.1016/j.coal.2009.01.002.

Kolker, Allan. 2023. “Rare Earth Elements and Critical Minerals in Coal and Coal Byproducts What Are Critical Minerals (CMs)?”

Landman, A. A. 2003. “CHAPTER 1 LITERATURE REVIEW OF FLY ASH.”

Mehmood, Mubashir. 2018. “Journal of Ecology & Natural Resources Rare Earth Elements- A Review.” (April). doi: 10.23880/JENR-16000128.

Mine, Haerwusu Surface, Jungar Coalfield, Shifeng Dai, Dan Li, Chen-lin Chou, Lei Zhao, Yong Zhang, and Deyi Ren. 2008. “Mineralogy and Geochemistry of Boehmite-Rich Coals : New Insights from The.” 74(6):185–202. doi: 10.1016/j.coal.2008.01.001.

MINERAL, By South Africa ’. s leading. 2010. “South Africa in the Global Rare Earth Sector.” 2005.

Miod, Michelle Christine. 2008. “The Determination of Heavy Metals in Coal Ash.” 14.

Mketo, Nomvano, Philiswa N. Nomngongo, and J. Catherine Ngila. 2014. “A Single-Step Microwave-Assisted Acid Extraction of Total Sulphur in Coal Samples Followed by ICP-OES Determination.” *Analytical*

Methods 6(21):8505–12. doi: 10.1039/c4ay01437e.

Mketo, Nomvano, Philiswa N. Nomngongo, and J. Catherine Ngila. 2016. “An Innovative Microwave-Assisted Digestion Method with Diluted Hydrogen Peroxide for Rapid Extraction of Trace Elements in Coal Samples Followed by Inductively Coupled Plasma-Mass Spectrometry.” *Microchemical Journal* 124:201–8. doi: 10.1016/j.microc.2015.08.010.

Ostrovnaya, Tatyna M., Leslie F. Petrik, and Marina V Frontasyeva. 2013. “ELEMENTAL COMPOSITION OF FLY ASH : A COMPARATIVE STUDY USING NUCLEAR AND RELATED ANALYTICAL TECHNIQUES.” 18:19–29. doi: 10.2478/cdem-2013-0014.

Paper, Professional. 1802. “Rare-Earth Elements Chapter O of Critical Mineral Resources of the United States — Economic and Environmental Geology and Prospects for Future Supply Professional Paper 1802 – O U . S . Department of the Interior.”

Peramaki, Siiri. 2006. *Method Development for Determination and Recovery of Rare Earth Elements from Industrial Fly Ash*.

Peterson, Rick, Mike Heinrichs, Justin Glier, and Annie Lane. 2017. “Recovery of Rare Earth Elements from Coal Ash with a Recycling Acid Leach Process.”

Pillay, Letitia. 2016. “An Evaluation of Chromatographic Modes for the Determination of Rare Earth Elements in Geological Materials by HPLC-ICP-MS by Risa Bagwandin.” (March).

Reynolds-Clausen, Kelley, and Nico Singh. 2019. “South Africa’s Power Producer’s Revised Coal Ash Strategy and Implementation Progress.” *Coal Combustion and Gasification Products* 11(1):1–10. doi:

10.4177/CCGP-D-18-00015.1.

Robert J. Weber , David J. Reisman. 2012. “Rare Earth Elements : A Review of Production , Processing , Recycling , and Associated Environmental Issues Rare Earth Elements : A Review of Production , Processing , Recycling , and Associated Environmental Issues.” *United States Environmental Protection Agency* (December):1–21.

Robinson, Philip, Neville C. Higgins, and George A. Jenner. 1986. “Determination of Rare-Earth Elements, Yttrium and Scandium in Rocks by Anion Exchange-X-Ray Fluorescence Technique.” *Chemical Geology* 55(1–2):121–37. doi: 10.1016/0009-2541(86)90132-4.

Sastri, V. S., J. C. G. Bünzli, V. R. Rao, G. V. S. Rayudu, and J. R. Perumareddi. 2003. “MODERN ASPECTS OF RARE EARTHS AND THEIR COMPLEXES.” *Modern Aspects of Rare Earths and Their Complexes* v–vi. doi: 10.1016/b978-044451010-5/50014-6.

Savic, Dejan. 2008. “Optimization of Microwave-Assisted Acid Digestion Method for Determination of Trace Elements in Coal and Coal Fly Ash.”

Schramm, Rainer. 2016. “Use of X-Ray Fluorescence Analysis for the Abstract :” 1–17. doi: 10.1515/psr-2016-0061.

Schulz, Bernhard, Gerhard Merker, and Jens Gutzmer. 2019. “Automated SEM Mineral Liberation Analysis (MLA) with Generically Labelled EDX Spectra in the Mineral Processing of Rare Earth Element Ores.” *Minerals* 9(9). doi: 10.3390/min9090527.

Scott, Clint, Amrika Deonarine, Allan Kolker, Monique Adams, and James Holland. 2015. “Size Distribution of Rare Earth Elements in Coal Ash.”

Shifeng, Weiguo Zhang, Vladimir V Seredin, Colin R. Ward, James C.

Hower, Weijiao Song, Xibo Wang, Xiao Li, Lixin Zhao, Huan Kang, Licai Zheng, Peipei Wang, and Dao Zhou. 2013. “International Journal of Coal Geology Factors Controlling Geochemical and Mineralogical Compositions of Coals Preserved within Marine Carbonate Successions : A Case Study from the Heshan Coal Fi Eld , Southern China.” *International Journal of Coal Geology* 109–110:77–100. doi: 10.1016/j.coal.2013.02.003.

Shikwambana, Lerato, Paidamwoyo Mhangara, and Nkanyiso Mbatha. 2020. “Trend Analysis and First Time Observations of Sulphur Dioxide and Nitrogen Dioxide in South Africa Using TROPOMI/Sentinel-5 P Data.” *International Journal of Applied Earth Observation and Geoinformation* 91(September):102130. doi: 10.1016/j.jag.2020.102130.

Simpson, John. 2020. “Coal Combustion Products.” (2).

Smoli, Adam, Marek Stempin, and Natalia Howaniec. 2016. “Spectrochimica Acta Part B Determination of Rare Earth Elements in Combustion Ashes from Selected Polish Coal Mines by Wavelength Dispersive X-Ray Fl Uorescence Spectrometry.” 116:63–74. doi: 10.1016/j.sab.2015.12.005.

Taggart, Ross K., James C. Hower, and Heileen Hsu-Kim. 2018. “Effects of Roasting Additives and Leaching Parameters on the Extraction of Rare Earth Elements from Coal Fly Ash.” *International Journal of Coal Geology* 196(February):106–14. doi: 10.1016/j.coal.2018.06.021.

Tuan, Lai Quang, Thriveni Thenepalli, Ramakrishna Chilakala, Hong Ha Thi Vu, Ji Whan Ahn, and Jeongyun Kim. 2019. “Leaching Characteristics of Low Concentration Rare Earth Elements in Korean (Samcheok) CFBC Bottom Ash Samples.” *Sustainability (Switzerland)* 11(9). doi:

10.3390/su11092562.

Twardowska, Irena, and Sebastian Stefaniak. 2006. “Coal and Coal Combustion Products: Prospects for Future and Environmental Issues.” *Coal Combustion Byproducts and Environmental Issues* 13–20. doi: 10.1007/0-387-32177-2_2.

Tyler, Geoff, and Horiba Group. n.d. “ICP-OES , ICP-MS and AAS Techniques Compared.” (3).

Vilakazi, Amanda Qinisile, Sehliselo Ndlovu, Liberty Chipise, and Alan Shemi. 2022. “The Recycling of Coal Fly Ash : A Review on Sustainable Developments and Economic Considerations.” 1–32.

Wagner, Nicola Jane, and Arnold Matiane. 2018a. “International Journal of Coal Geology Rare Earth Elements in Select Main Karoo Basin (South Africa) Coal and Coal Ash Samples.” *International Journal of Coal Geology* 196(July):82–92. doi: 10.1016/j.coal.2018.06.020.

Wagner, Nicola Jane, and Arnold Matiane. 2018b. “Rare Earth Elements in Select Main Karoo Basin (South Africa) Coal and Coal Ash Samples.” *International Journal of Coal Geology* 196:82–92. doi: 10.1016/j.coal.2018.06.020.

Wdowin, Magdalena. 2015. “Coal Fly Ash as a Resource for Rare Earth Elements.” (January). doi: 10.1007/s11356-015-4111-9.

Wojciech., Franus, Wiatros-Motyka. Małgorzata M., and Wdowin Magdalena. 2015. “Coal Fly Ash as a Resource for Rare Earth Elements.” *Environmental Science and Pollution Research* 22(12):9464–74. doi: 10.1007/s11356-015-4111-9.

Yu, D. N. Konshina M., and Burylin R. Anashkin. 2019. “Solid - Phase

Extraction with Injection of Modified Silica Gel Slurries into ETAAS for Determination of Cu (II), Hg (II), Pd (II).” *International Journal of Environmental Science and Technology* 16(7):2885–94. doi: 10.1007/s13762-018-1917-2.

Zawisza, Beata, Katarzyna Pytlakowska, Barbara Feist, Marzena Polowniak, Andrzej Kita, and Rafal Sitko. 2011. “Determination of Rare Earth Elements by Spectroscopic Techniques: A Review.” *Journal of Analytical Atomic Spectrometry* 26(12):2373–90.

Zhang, Wencai, Xinbo Yang, and Rick Q. Honaker. 2018. “Association Characteristic Study and Preliminary Recovery Investigation of Rare Earth Elements from Fire Clay Seam Coal Middlings.” *Fuel* 215(November 2017):551–60. doi: 10.1016/j.fuel.2017.11.075.

Appendix

Appendix 1

Microwave digestion Report

Anton Paar Multiwave 5000

Experiment Report

Serial Number:	84150011	Software Version:	1.12.21.0
Configuration:	00100010		
Name:	-	Location:	-

Processing Protocol

Name:	20230620-1712_12	Date:	06/20/2023 17:13:12
User at start:	Administrator		
Consecutive Number	12		
Unique ID:	f57ef78a-b991-4dfb-a9f6-e0a8405a64d6		

Graph

--- IR Vessel 1 --- Control Temperature --- Power

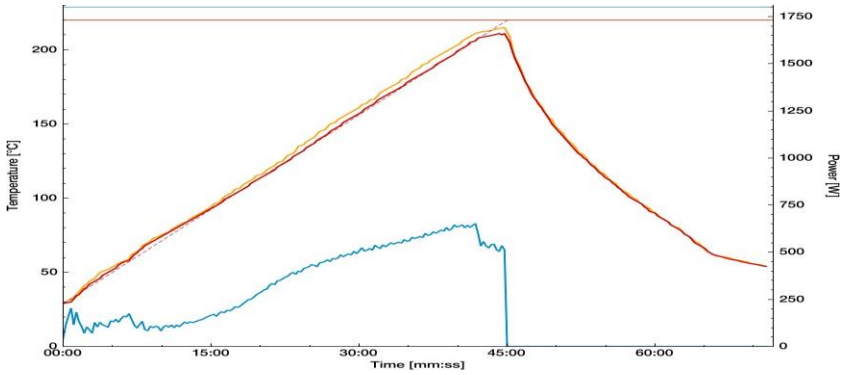

Vessels 1 - 20

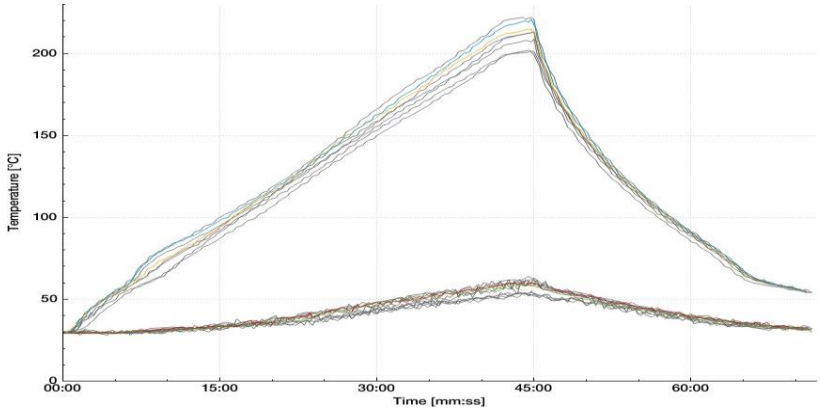

Method Settings

Name:	REES DEV	Rotor:	Rotor 20SVT50
Application Group:	Acid Digestion	Category:	Ores. Minerals
Program Type:	Temperature	Vessels:	8
Cooling temperature [°C]	55	Cooling fan level	3
Temperature Control Mode	Average		

Limits

Power Limit [W]	1800
T-Limit [°C]	220

Steps

		Temperature	Time	
1	Time	220	00:45:00	2

Sample Documentation

-

Recipe

HCL.HNO3 & HF

Experiment Result

Status:	Success		
Total Runtime: [hh:mm:ss]	01:11:32	Controller State	

Maxima

Max. Internal T [°C]	211.9		
Max. power [W]	652		
T Vessel 1 [°C]	215	T Vessel 2 [°C]	60
T Vessel 3 [°C]	221	T Vessel 4 [°C]	59
T Vessel 5 [°C]	54	T Vessel 6 [°C]	213
T Vessel 7 [°C]	64	T Vessel 8 [°C]	213
T Vessel 9 [°C]	62	T Vessel 10 [°C]	54
T Vessel 11 [°C]	209	T Vessel 12 [°C]	62
T Vessel 13 [°C]	222	T Vessel 14 [°C]	63
T Vessel 15 [°C]	54	T Vessel 16 [°C]	201
T Vessel 17 [°C]	61	T Vessel 18 [°C]	202
T Vessel 19 [°C]	60	T Vessel 20 [°C]	55
Max. Tmag1 [°C]	81	Max. Tmag 2 [°C]	59
Max. Current [A]	9.8		

Appendix 2

Calibration curves for REE elements in the instrument:

Instrument Name	Serial Number
iCAP Q	03334R

LabBook	LabBook Path
REEs 11.03.2023.imexp	_Application Data\Workspace\LabBooks

151Eu (STD)

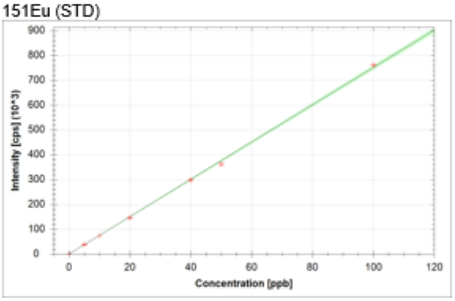

f(x) = 7511.9680*x + 677.1498
R² = 0.9992
BEC = 0.090 ppb
LoD = 0.0136 ppb

151Eu (KED)

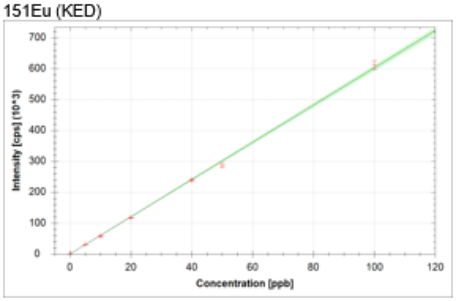

f(x) = 6019.6734*x + 513.7813
R² = 0.9988
BEC = 0.085 ppb
LoD = 0.0136 ppb

153Eu (STD)

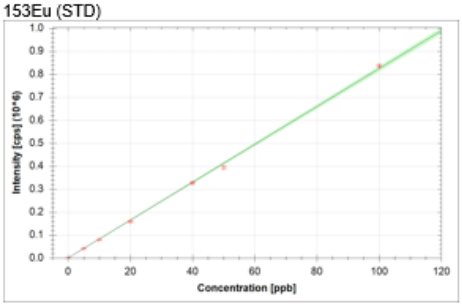

f(x) = 8241.3884*x + 795.7597
R² = 0.9989
BEC = 0.097 ppb
LoD = 0.0044 ppb

153Eu (KED)

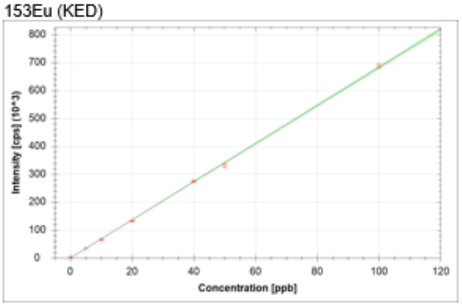

f(x) = 6824.9441*x + 543.3533
R² = 0.9995
BEC = 0.080 ppb
LoD = 0.0034 ppb

157Gd (STD)

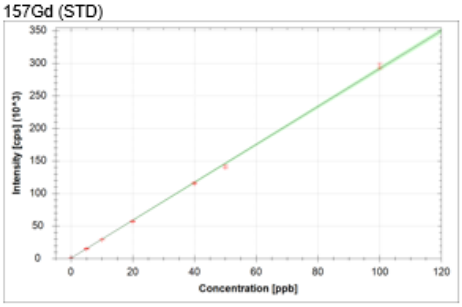

f(x) = 2911.1076*x + 709.5309
R² = 0.9993
BEC = 0.244 ppb
LoD = 0.0306 ppb

157Gd (KED)

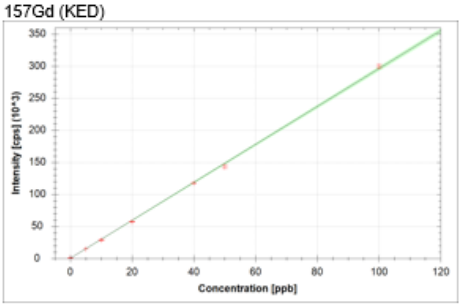

f(x) = 2956.9598*x + 579.7814
R² = 0.9993
BEC = 0.196 ppb
LoD = 0.0070 ppb

89Y (STD)

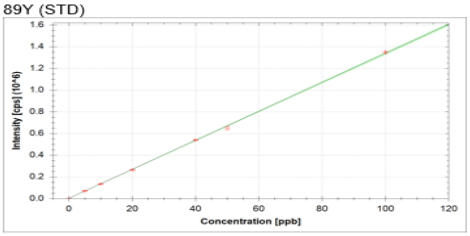

f(x) = 13355.0384*x + 3156.3357
R² = 0.9995
BEC = 0.236 ppb
LoD = 0.0150 ppb

89Y (KED)

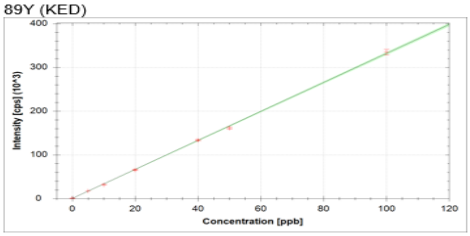

f(x) = 3312.5790*x + 638.9090
R² = 0.9995
BEC = 0.193 ppb
LoD = 0.0403 ppb

139La (STD)

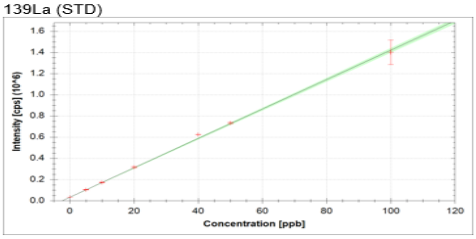

f(x) = 13870.3807*x + 33136.6307
R² = 0.9987
BEC = 2.389 ppb
LoD = 0.0866 ppb

139La (KED)

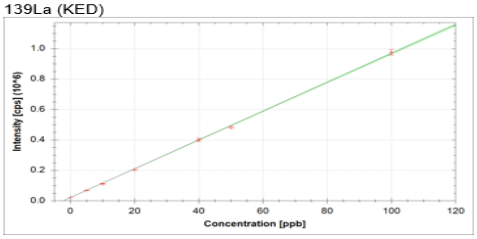

f(x) = 9464.1751*x + 21077.2646
R² = 0.9995
BEC = 2.227 ppb
LoD = 0.0478 ppb

174Yb (STD)

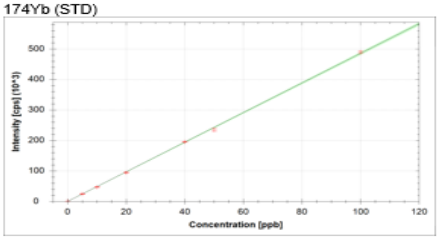

f(x) = 4852.9728*x + 290.8244
R² = 0.9995
BEC = 0.060 ppb
LoD = 0.0171 ppb

174Yb (KED)

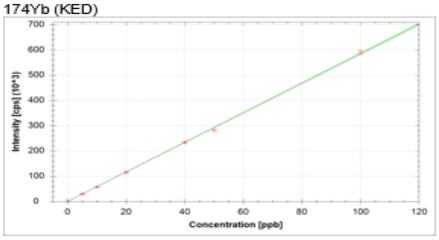

f(x) = 5851.7230*x + 323.3428
R² = 0.9994
BEC = 0.055 ppb
LoD = 0.0101 ppb

175Lu (STD)

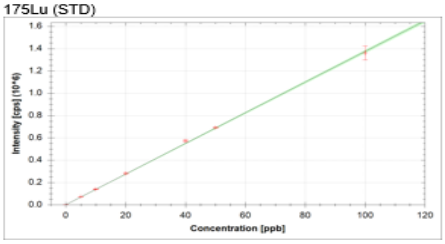

f(x) = 13739.7301*x + 698.9816
R² = 0.9994
BEC = 0.051 ppb
LoD = 0.0016 ppb

175Lu (KED)

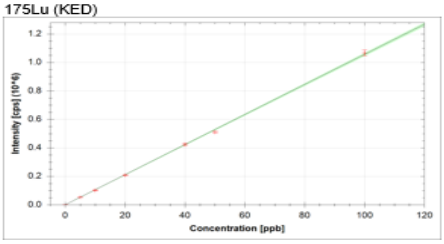

f(x) = 10559.2642*x + 467.4802
R² = 0.9994
BEC = 0.044 ppb
LoD = 0.0089 ppb

146Nd (STD)

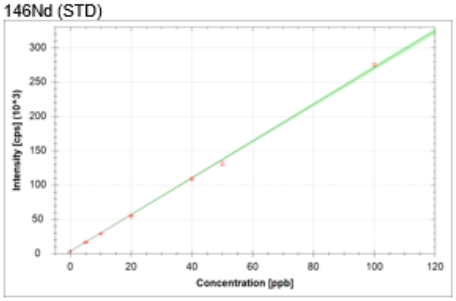

f(x) = 2676.2262*x + 3398.0749
R^2 = 0.9989
BEC = 1.270 ppb
LoD = 0.0279 ppb

146Nd (KED)

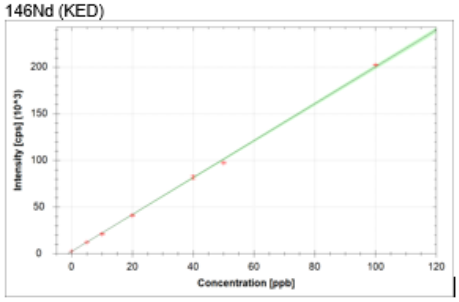

f(x) = 1978.0939*x + 2436.8000
R^2 = 0.9992
BEC = 1.232 ppb
LoD = 0.0709 ppb

147Sm (STD)

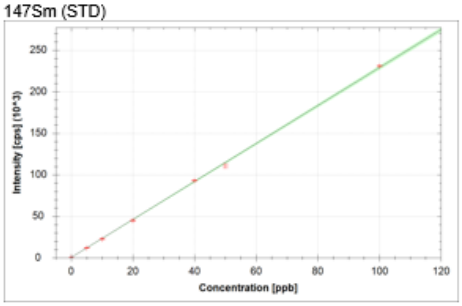

f(x) = 2284.2157*x + 672.8939
R^2 = 0.9994
BEC = 0.295 ppb
LoD = 0.0342 ppb

147Sm (KED)

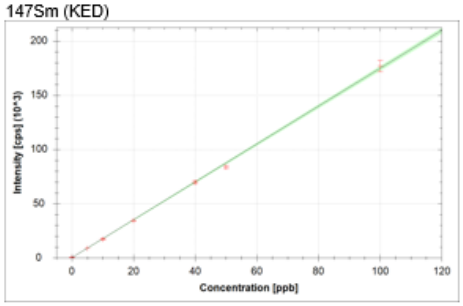

f(x) = 1745.9414*x + 335.4858
R^2 = 0.9991
BEC = 0.192 ppb
LoD = 0.0166 ppb

149Sm (STD)

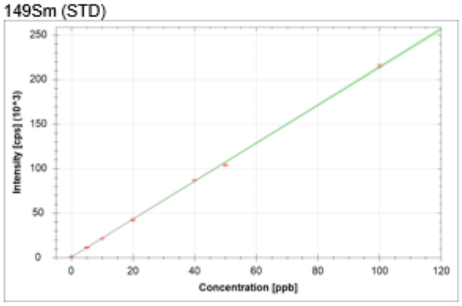

f(x) = 2134.9397*x + 541.4592
R^2 = 0.9995
BEC = 0.254 ppb
LoD = 0.0246 ppb

149Sm (KED)

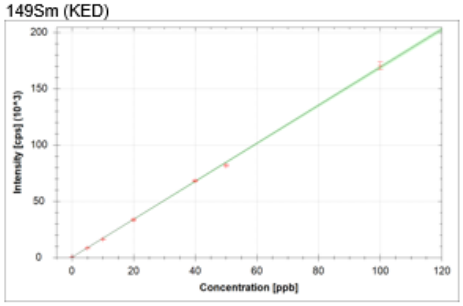

f(x) = 1687.8763*x + 339.5195
R^2 = 0.9995
BEC = 0.201 ppb
LoD = 0.0185 ppb

Appendix 3

REFERENCE MATERIAL CERTIFICATE CGL 111

MONGOLIA
CENTRAL GEOLOGICAL LABORATORY

REFERENCE MATERIAL CERTIFICATE
(Certified reference material)

CGL 111
TRM-2 (RARE EARTH ORE)

Certified values

No.	Oxide/ Element	Unit	CV [1]	±Δ A (P=0.95)	N [3]
1.	SiO_2	% m/m	14.86	0.17	21
2.	TiO_2	% m/m	0.15	0.04	20
3.	Al_2O_3	% m/m	2.47	0.10	21
4.	Fe_2O_3	% m/m	13.45	0.26	21
5.	FeO	% m/m	0.14	0.03	13
6.	MnO	% m/m	0.14	0.01	22
7.	MgO	% m/m	0.50	0.02	22
8.	CaO	% m/m	25.51	0.50	21
9.	Na_2O	% m/m	0.92	0.05	19
10.	K_2O	% m/m	0.91	0.08	17
11.	P_2O_5	% m/m	19.26	0.28	19
12.	SO_3	% m/m	4.58	0.32	24
13.	LOI*	% m/m	6.78	0.22	14
14.	As	mg/kg	155.83	26.58	12
15.	Ba	mg/kg	917	58	12
16.	CO_2	% m/m	1.04	0.07	6
17.	Co	mg/kg	32.46	6.03	16
18.	Ce	% m/m	2.90	0.12	19
19.	Cu	mg/kg	128	58	20
20.	Dy	mg/kg	206	32	9
21.	Eu	mg/kg	211.60	16.20	11
22.	Er	mg/kg	79.50	8.50	9
23.	Ho	mg/kg	36.60	7.40	9
24.	Gd	mg/kg	553	83	11
25.	La	% m/m	1.93	0.10	25
26.	Lu	mg/kg	7.64	1.08	6
27.	Nd	% m/m	0.88	0.08	20
28.	Ni	mg/kg	70.80	11.20	14
29.	Pb	% m/m	0.11	0.014	16
30.	Pr	% m/m	0.28	0.03	17
31.	Rb	mg/kg	43	10	10

No.	Oxide/ Element	Unit	CV [1]	$\pm\Delta_A$ (P=0.95) [2]	N [3]
32.	Sm	% m/m	0.09	0.03	12
33.	Sr	% m/m	2.24	0.095	11
34.	$\sum TR_2O_3$	% m/m	7.56	0.25	13
35.	Tb	mg/kg	54.60	14.20	8
36.	Th	mg/kg	217.58	40.42	15
37.	V	mg/kg	138.6	18.9	8
38.	Y	mg/kg	959	40	14
39.	Yb	mg/kg	54.52	5.24	10
40.	Zn	% m/m	0.06	0.004	21

[1] Certified value (CV) – based on a minimum of 6 results
[2] Confidence interval ($\pm\Delta_A$) at 95% level
[3] Number of datasets (N)
* LOI – Loss on Ignition

Additional information

No.	Oxide/ Element	Unit	IV[4]
1.	CaF_2	% m/m	32.90
2.	H_2O^-*	% m/m	0.67
3.	F	% m/m	1.89
4.	Mo	mg/kg	23.86

[4] Indicative value (IV) – one certification criteria is not fulfilled
* H_2O^- - moisture

Description of the sample

The starting material was a bulk of Rare earth ore collected from the Mushgia khudag deposit at Umnogobi province, Mongolia. The sample was collected by the Central Geological Laboratory (CGL) Ulaanbaatar, Mongolia. Sample preparation and bottling was executed in 1998 by the CGL.

The mineral composition of the material has been determined to be:

Minerals	Percentage (% m/m)
Apatite	48.6
Secondary phosphate	11.6
Hydrous ferric oxide	16.8
Quartz	10.1
Gypsum	5.5
Calcite	2.1
Sericite	3.4
Celestine	1.5
Fluorite	0.8
Epidote, pyrite	few particles

Appendix 4

REFERENCE MATERIAL CERTIFICATE cgl 124

Reg. No: **USZ 42-2006**

MONGOLIA
CENTRAL GEOLOGICAL LABORATORY

CERTIFICATE OF ANALYSIS

Certified Reference Material "TRLK"

Rare earth ore "CGL 124"

Certified values (CV) and their confidence interval ($\pm\Delta_A$)

No.	Oxides/ Elements	Unit	CV	$\pm\Delta_A$	N
1.	SiO_2	%	11.86	0.15	28
2.	TiO_2	%	0.20	0.012	30
3.	Al_2O_3	%	2.72	0.13	30
4.	Fe_2O_3	%	5.71	0.17	28
5.	CaO	%	32.68	0.40	29
6.	MgO	%	2.78	0.05	26
7.	MnO	%	1.67	0.05	28
8.	Na_2O	%	0.25	0.03	25
9.	K_2O	%	1.55	0.05	23
10.	P_2O_5	%	0.22	0.01	26
11.	Loss on ignition	%	30.56	0.12	22
12.	CO_2	%	29.00	0.33	15
13.	As	mg/kg	224	24	11
14.	Ba	mg/kg	307	10	10
15.	Ce	%	2.76	0.05	16
16.	Co	mg/kg	7.89	0.81	10
17.	Cu	mg/kg	27.37	6.43	18
18.	Dy	mg/kg	57.63	11.63	8
19.	Eu	mg/kg	87.22	8.68	9
20.	Ho	mg/kg	7.86	1.72	7
21.	La	%	2.11	0.11	17
22.	Li	mg/kg	21.78	2.23	9
23.	Mo	mg/kg	34.40	3.41	10
24.	Nb	mg/kg	31	4.54	8
25.	Nd	%	0.65	0.03	16
26.	Ni	mg/kg	13.18	3.50	14
27.	Pb	%	0.16	0.007	23

Page 1 of 5

No.	Oxides/ Elements	Unit	CV	$\pm\Delta_A$	N
28.	Pr	%	0.23	0.03	14
29.	Rb	mg/kg	67.12	3.91	17
30.	Sm	mg/kg	539	62	15
31.	Sr	%	0.49	0.04	22
32.	Th	mg/kg	946	51	14
33.	V	mg/kg	115	14.92	10
34.	Y	mg/kg	167	20	11
35.	Yb	mg/kg	17.85	1.92	8
36.	Zn	mg/kg	469	21	24
37.	ΣTR_2O_3	%	8.27	0.25	10

Information values (IV)

No.	Oxides/ Elements	Unit	IV
1	FeO	%	0.08
2	SO_3	%	0.14
3	H_2O^-	%	0.19
4	H_2O^+	%	2.03
5	F	%	1.61
6	Au	mg/kg	0.46
7	Bi	mg/kg	8.7
8	Cr	mg/kg	33.56
9	Cs	mg/kg	54.55
10	Er	mg/kg	23.88
11	Gd	mg/kg	295
12	Sc	mg/kg	15.17
13	Tb	mg/kg	45
14	U	mg/kg	51.4
15	W	mg/kg	18.71
16	Zr	mg/kg	136

Classification criteria

CV – certified value satisfying certification criteria
IV - not certified value not satisfying certification criteria

Appendix 5

REFERENCE MATERIAL CERTIFICATE AMIS0276

African Mineral Standards

MATRIX REFERENCE MATERIALS

Tel: +27 (0) 11 923 0800. Fax: +27 (0) 11 392 4715. web: www.amis.co.za

11 Gewel Street (off Hulley Road). D1 Isando Business Park. Kempton Park. 1609
P.O. Box 856. Isando. 1600. Gauteng. South Africa. a division of the Set Point Group

AMIS0276

Certified Reference Material

Rare Earth Elements TRE Project. Madagascar

Analysis certificate

Recommended Concentrations and Limits[1. 2.]

(at two standard deviations)

Certified Concentrations

Ce FUS	215	±	17	ppm
Dy FUS	8.4	±	0.7	ppm
Er FUS	5.4	±	0.4	ppm
Gd FUS	8.4	±	1.2	ppm
Ho FUS	1.8	±	0.1	ppm
La FUS	75.4	±	5.9	ppm
La M/ICP	76.6	±	8.1	ppm

Nb Fus	107	±	11	ppm
Nb M/ICP	108	±	7	ppm
Nd FUS	53.8	±	4.3	ppm
Pr FUS	15.3	±	1.1	ppm
Sm FUS	9.7	±	0.9	ppm
Sr M/ICP	16.6	±	1.7	ppm
U Fus	6.9	±	0.5	ppm
Yb FUS	5.4	±	0.5	ppm
Yb M/ICP	3.4	±	0.3	ppm
Specific Gravity	2.58	±	1.2	

Provisional Concentrations

Ce M/ICP	208	±	42	ppm
Eu FUS	1.37	±	0.16	ppm
Lu FUS	8.3	±	0.1	ppm
Lu M/ICP	0.5	±	0.1	ppm
Sc M/ICP	13.1	±	1.6	ppm
Sr FUS	17.9	±	4.2	ppm
Tb FUS	1.4	±	0.2	ppm
Tb M/ICP	1.2	±	0.1	ppm
Th Fus	34.7	±	5.3	ppm
Th M/ICP	27.9	±	4.7	ppm
Tm FUS	0.81	±	0.08	ppm
U M/ICP	4.90	±	1.10	ppm
Y FUS	46.6	±	6.0	ppm

Major Element Recommended Concentrations and Limits

(at two Standard Deviation)

Certified Concentrations

Al_2O_3	23.9	±	0.4	%
CaO	0.3	±	0.01	%
Fe_2O_3	9.7	±	0.2	%
K_2O	1.7	±	0.04	%
MgO	0.6	±	0.02	%
MnO	0.1	±	0.01	%
P_2O_5	0.090	±	0.002	%
SiO_2	51.4	±	0.8	%
TiO_2	1.0	±	0.04	%
LOI	10.2	±	0.3	%

Provisional Concentrations

Cr_2O_3	0.03	±	0.01	%
Na_2O	0.3	±	0.06	%